




Temperature Profiles in
Subcooled Nucleate Boiling

by

Jim Richard Wiebe, B. Sc.

McMASTER UNIVERSITY LIBRARY
THESIS T 731647
Temperature profiles in subcoo C.2



3 9005 0472 3910 2

TEMPERATURE PROFILES
IN
SUBCOOLED NUCLEATE BOILING

MASTER OF ENGINEERING (1970)
(Mechanical Engineering)

McMASTER UNIVERSITY
Hamilton, Ontario

TITLE: TEMPERATURE PROFILES IN SUBCOOLED NUCLEATE
BOILING

AUTHOR: Jim Richard Wiebe, B.Sc.(M.E)
(University of Manitoba, Winnipeg)

SUPERVISOR: Dr. R. L. Judd

NUMBER OF PAGES: viii, 92

SCOPE AND CONTENTS:

An experimental study of temperature profiles in the near vicinity of a horizontal copper surface on which water was boiled is reported in this thesis. A series of three tests is reported for heat fluxes of 20,000, 50,000 and 100,000 BTU/HRFT² respectively. Four levels of subcooling were achieved in each series in the range of $0^{\circ}\text{F} < \theta_{\text{sub}} < 105^{\circ}\text{F}$. Using the superheat-layer thickness as defined by Han and Griffith, results are reported indicating an increase in superheat-layer thickness for an increase in the degree of subcooling at a constant heat flux and a reverse effect for an increase in heat flux for a constant degree of subcooling.

In addition, five tests are reported in which incipience of boiling was achieved. Using this data,

Hsu's mathematical model for predicting bubble nucleation is tested. In general, good agreement is found between the Hsu model and the experimental data.

°

ACKNOWLEDGEMENTS

The author gratefully acknowledges the assistance and support of Dr. R. L. Judd who provided guidance in the planning and performing of this experimental study.

The financial support provided by the National Research Grant A4362 is gratefully acknowledged.

TABLE OF CONTENTS

<u>TEXT</u>		<u>PAGE</u>
1.	Introduction	1
2.	Literature Survey	2
3.	Experimental Apparatus	12
	3.1 Design Criteria	12
	3.2 Boiler Assembly	12
	3.3 Thermocouples	18
	3.4 Thermocouple Probe and Traverse Mechanism	21
	3.5 Power Circuitry and Measurement	27
	3.6 Temperature Measuring System	27
4.	Test Conditions	31
5.	Test Procedure	33
6.	Data Reduction	36
7.	Results	39
8.	Discussion	46
9.	Conclusions	58
10.	Nomenclature	59
11.	References	66
 <u>APPENDIX</u>		
A.	Estimate of Heat Loss	69

<u>APPENDIX</u>	<u>PAGE</u>
B. Extrapolation of the Axial Temperature Gradient in the Heater Block	79
C. Bulk Liquid Temperature	81
D. Design of Thermocouple Probe	83
E. Tabulation of Data	87
F. Uncertainty Analysis	88

LIST OF ILLUSTRATIONS

<u>FIGURE NO.</u>	<u>TITLE</u>	<u>PAGE</u>
1	Section of Boiler Vessel	13
2	Location of Thermocouples in Neck of Copper Heating Block	16
3	Thermocouple Assembly	20
4	Micro-Thermocouple and Traverse Mechanism	23
5	Power Circuit Diagram	28
6	Thermocouple Circuit Diagram	29
7	Characteristic Boiling Curve	40
8	Variation of Wall Superheat with Bulk Subcooling	41
9	Temperature Profiles at $Q/A = 20,000 \text{ BTU/HRFT}^2$	42
10	Temperature Profiles at $Q/A = 50,000 \text{ BTU/HRFT}^2$	43
11	Temperature Profiles at $Q/A = 100,000 \text{ BTU/HRFT}^2$	44
12	Temperature Profiles at Incipience of Boiling Condition	45
13	Determination of Superheat Layer Thickness	48
14	Incipience of Boiling Heat Transfer Data	52

<u>FIGURE NO.</u>	<u>TITLE</u>	<u>PAGE</u>
15	Boundary Layer Thickness Correlation	53
16	K_{eff}/K Correlation	56
17	Test Facility	63
18	Precision Potentiometer and Related Instruments	64
19	Heat Flux Correction Curve	71
20	Location of Thermocouples Used in Determining Heat Loss	74
21	Bulk Liquid Temperature Profiles	82

LIST OF TABLES

<u>TABLE</u>		<u>PAGE</u>
I	Test Conditions	32
II	Tabulation of Data	87
III	Incipience of Boiling Data	88
IV	Uncertainty Analysis	90

1.

INTRODUCTION

Nucleate boiling is one of the most efficient modes of heat transfer in use today. Whereas in the past the limiting factor in heat exchanger design has usually been the mechanical design, currently the surface to liquid heat transfer resistance is the primary consideration. Thus, with the development of high power density equipment it has become increasingly important to utilize nucleate boiling. As a consequence, a better understanding of the nucleate boiling phenomena has been necessitated.

It has long been recognized that one of the most important parameters in nucleate boiling is the condition of the heating surface, characterized by the size, space and shape distribution of pits and scratches that constitute nucleation sites. Because of the small size of these sites it has been difficult to effectively describe them in order to incorporate surface condition in any relationship of surface superheat and heat flux. Adding to this difficulty is the fact that deposits from the bulk liquid may change the surface condition during prolonged boiling and may either enhance or detract from the boiling process.

Among the techniques used to describe and reproduce surface condition are micro-roughness measurements, photographic analysis and prescribed finishing processes. Another way which has been postulated to represent the surface condition is to relate the temperature distribution in the liquid during boiling to the condition of the surface at which boiling occurs. The micro-structure of the surface is thought to have a direct effect on the temperature distribution in the bulk liquid because of the effect which micro-structure has on active site density. If this is the case, surfaces can be identified with the temperature distribution they produce when boiling a given liquid. This hypothesis has not yet been proven, in as much as reliable information describing the temperature variation adjacent to a boiling surface is not readily available. If the hypothesis could be proven, it would seem reasonable to relate the temperature distribution adjacent to a boiling surface with the active nucleation site density.

2.

LITERATURE SURVEY

In 1931 Jakob and Fritz (1) first noticed the presence of a superheated boundary layer in boiling water. In this early investigation, a thermocouple probe was used to measure the temperature profile in the nucleate pool boiling water. The probe was large in comparison with the thickness of the superheated region which was found to be only a few millimeters thick and it was not possible to study the profile within the superheated region in any detail.

In 1960 Griffith and Wallis (2) made an attempt to predict bubble nucleation conditions by considering a single idealized conical cavity under thermodynamic equilibrium. A study of such a cavity determined that the minimum radius of curvature of the nucleus, corresponding to the minimum energy condition, was equal to the radius of the cavity mouth. The manner in which Griffith and Wallis related the radius of curvature of a nucleus and the liquid superheat is outlined below. Application of Gibbs equation for static mechanical and thermodynamic equilibrium results in

$$\Delta P = (P_v - P_l) = \frac{2\sigma}{r_c} \quad (1)$$

When the nucleus is at equilibrium, the pressure inside the nucleus P_v and the temperature of the vapour T_v must correspond to saturation conditions; that is the vapour must be at the saturation temperature corresponding to its pressure. In order that there be no net heat transfer across the vapour liquid interface, the liquid temperature T_l must be the same as the vapour temperature T_v . Therefore, the liquid surrounding the nucleus must be superheated. The Clapeyron equation can be used to relate the excess temperature in the liquid to the excess pressure in the nucleus. In finite difference form the equation is

$$\frac{\Delta P}{(T_w - T_{sat})} = \frac{h_{fg}}{T_w v_{fg}} \quad (2)$$

By combining Equation (1) and (2), ΔP can be eliminated bringing a relationship between liquid superheat and radius of curvature of the nucleus.

$$r = \frac{2\sigma T_w v_{fg}}{h_{fg}(T_w - T_{sat})} \quad (3)$$

Griffith and Wallis postulated that by substituting the radius of the cavity mouth, Equation (3) would predict the minimum temperature difference required to start bubble growth from a cavity.

A surface characterized by cavities of known size was used to test the prediction of wall superheat as given by Equation (3). A test was performed in which saturated liquid was boiled from a heated surface containing artificial cavities 0.002 inches in diameter. Wall superheat of 20°F was observed while Equation (3) predicted 3°F. Using the same surface Griffith and Wallis performed another test in uniformly superheated liquid and found ebullition from the surface to start at 3°F as predicted by Equation (3). These tests gave evidence that higher temperatures are required for nucleation in non-uniform temperature fields than in uniformly superheated liquids. It was also apparent that the Griffith and Wallis model did not describe bubble nucleation adequately.

In 1962 Hsu (3) developed an improved mathematical model in an attempt to predict bubble nucleation in a non-uniform temperature field. The model attempted to determine the relationship between cavity size and surface temperature and to predict the maximum and minimum sizes of potentially active nucleation sites.

In the model Hsu postulated that at the beginning of a cycle of bubble emission, relatively cool bulk liquid at temperature T_{∞} surrounded the

the nucleus at an active site. This cool liquid had replaced the liquid displaced by the previous bubble. As time progressed, the cool liquid was heated by transient conduction and its energy content increased. The thickness of the liquid layer heated in this way increased with time but not without limit in as much as the ultimate thermal layer thickness was governed by eddy diffusivity and turbulence which tended to hold the temperature constant at the bulk temperature T_∞ beyond a certain distance from the surface. Hsu then postulated the nucleus would not grow until the temperature of the surrounding liquid was such that a heat balance on the nucleus produced a net inflow of heat. When the thermal layer had grown to such an extent that this condition was satisfied, the nucleus would begin to grow.

Using this model Hsu developed an equation to predict the maximum and minimum radius for active cavities. For the case of constant surface temperature

$$r_{c \begin{matrix} \text{max} \\ \text{min} \end{matrix}} = \frac{\delta}{2C_1} \left[1 - \frac{\theta_{\text{sat}}}{\theta_w} + \left(\left(1 - \frac{\theta_{\text{sat}}}{\theta_w} \right)^2 - \frac{4AC_3}{\delta\theta_w} \right)^{1/2} \right] \quad (4)$$

Hsu explained that although it was necessary that

$r_{c_{\text{min}}} < r_c < r_{c_{\text{max}}}$ for a cavity to be active, this

condition was not a sufficient condition. In the case of two cavities, both with favourable geometry located very close to each other, the one with the shorter bubble emission cycle would be the active site. Hence, Equation (4) cannot be used to predict the total number of active sites even if the cavity size distribution for a surface were known, as all the sites within the range $r_{c_{\min}} < r_c < r_{c_{\max}}$ are not necessarily active. From Equation (4) Hsu derived a relationship for the incipience of boiling

$$\theta_{wo} = \theta_{sub} + \frac{2AC_3}{\delta} + \left[(2\theta_{sub} + \frac{2AC_3}{\delta}) (\frac{2AC_3}{\delta}) \right]^{1/2} \quad (5)$$

An important parameter in Equation (4) and (5) is δ , the limiting thermal layer thickness.

One way in which the Hsu model can be tested is to evaluate Equation (5) using incipient boiling conditions. At this condition, only one cavity size is active and for this reason, cavity size does not appear in Equation (5). One value of δ then characterizes the superheated temperature profile in the bulk liquid.

Hsu used Equation (5) to predict δ from experimental data of incipient boiling and having obtained a numerical value, proceeded by assuming it did not change significantly with heat flux. Using this assumption, Hsu was able to demonstrate that

Equation (5) predicts with some confidence the incipience of boiling for various levels of bulk liquid subcooling and pressures.

In 1965 Marcus and Dropkin (4) carried out an extensive investigation of the superheated boundary layer above a nickel plated copper surface in saturated nucleate pool boiling water. These investigators developed a technique for manufacturing 0.001 inch diameter thermocouple probes which enabled them to study the superheated region in some detail. An important finding of their investigation was that in the very near proximity of the heated surface, the temperature profiles were essentially linear. In general, the value of the superheated boundary layer thickness decreased with an increase in heat flux. Also according to Marcus and Dropkin the "extrapolated superheat layer thickness" defined as the distance from the surface at which an extrapolation of the linear portion of the temperature profile intersected the bulk temperature line, is primarily a function of the heat transfer coefficient. Marcus and Dropkin postulated that the correlation of heat transfer coefficient and "extrapolated superheat layer thickness" could be broken into two regimes corresponding to the discrete bubble

and first transition regimes wherein bubbles depart without interaction and bubble coalescence begins respectively.

The instantaneous temperature at a given point in the superheated boundary layer was found to fluctuate rapidly. The amplitude of the temperature fluctuation was noticed to reach a maximum a short distance from the surface and then to decrease to a very small value in the immediate vicinity of the surface. Marcus and Dropkin postulated that the surface acts as a smoothing agent inhibiting agitation in the liquid and thus the temperature fluctuations are damped.

In 1968, Lippert and Dougall (5) undertook an investigation similar to that of Marcus and Dropkin in that temperature profiles were measured in the superheated layer during pool boiling. In this case a 0.005 inch diameter thermocouple probe was used and Freon 113, methyl alcohol and water were boiled on a copper heating surface. Lippert and Dougall reproduced Marcus and Dropkin's results for water in regard to the relationship of the "extrapolated superheat layer thickness" δ to the convection coefficient h . The correlation of δ with h shifted with a change in fluid thus indicating a dependence upon fluid properties. All tests were

done with the bulk liquid at or near saturation temperatures.

In 1968 Bobst and Colver (6) reported measurements of the superheated boundary layer in saturated pool boiling and verified the previous work of Marcus and Dropkin and Lippert and Dougall. In addition, the authors demonstrated the existence of a third region in the correlation of convection coefficient with "extrapolated superheat layer thickness" corresponding to the range in which significant bubble coalescence takes place.

Recent work in the measurement of superheated boundary layer was done by Judd (7). In this investigation Freon 113 was boiled on a glass plate coated with an electrically conducting oxide and a 0.001 inch diameter thermocouple probe was used. Subcooling, acceleration and heat flux were varied so as to show the individual effects of these parameters. In accordance with previous investigations, Judd found the superheated boundary layer decreased with an increase of heat flux. Furthermore, the superheated boundary layer was found to decrease with acceleration and increase with subcooling.

To this author's knowledge, no other investigation has been performed to determine the effect of subcooling on the superheated boundary layer in nucleate pool boiling of water. It was to this end that the current investigation was directed.

3.

EXPERIMENTAL APPARATUS

It is convenient to consider the test apparatus in six sections; the apparatus design criteria, the boiler assembly, thermocouples, the thermocouple probe and traverse mechanism, the power circuitry and measurement and the temperature measuring system.

3.1. DESIGN CRITERIA

The test apparatus was designed to be capable of:

1. Boiling fluids up to a maximum heat flux of 250,000 BTU/HRFT².
2. Subcooling the bulk liquid by at least 50°F at the maximum heat flux condition.
3. Pressurization up to 100 psig.
4. Measuring temperature profiles in the bulk liquid in the near proximity of the boiling surface.

3.2. BOILER ASSEMBLY

A sectional view of the complete boiler assembly is presented in Figure (1). The basic vessel consisted of an 18 inch length of 8 inch schedule 40 stainless steel pipe with 3/4 inch stainless steel flanges welded on the outside at the ends of the pipe. The

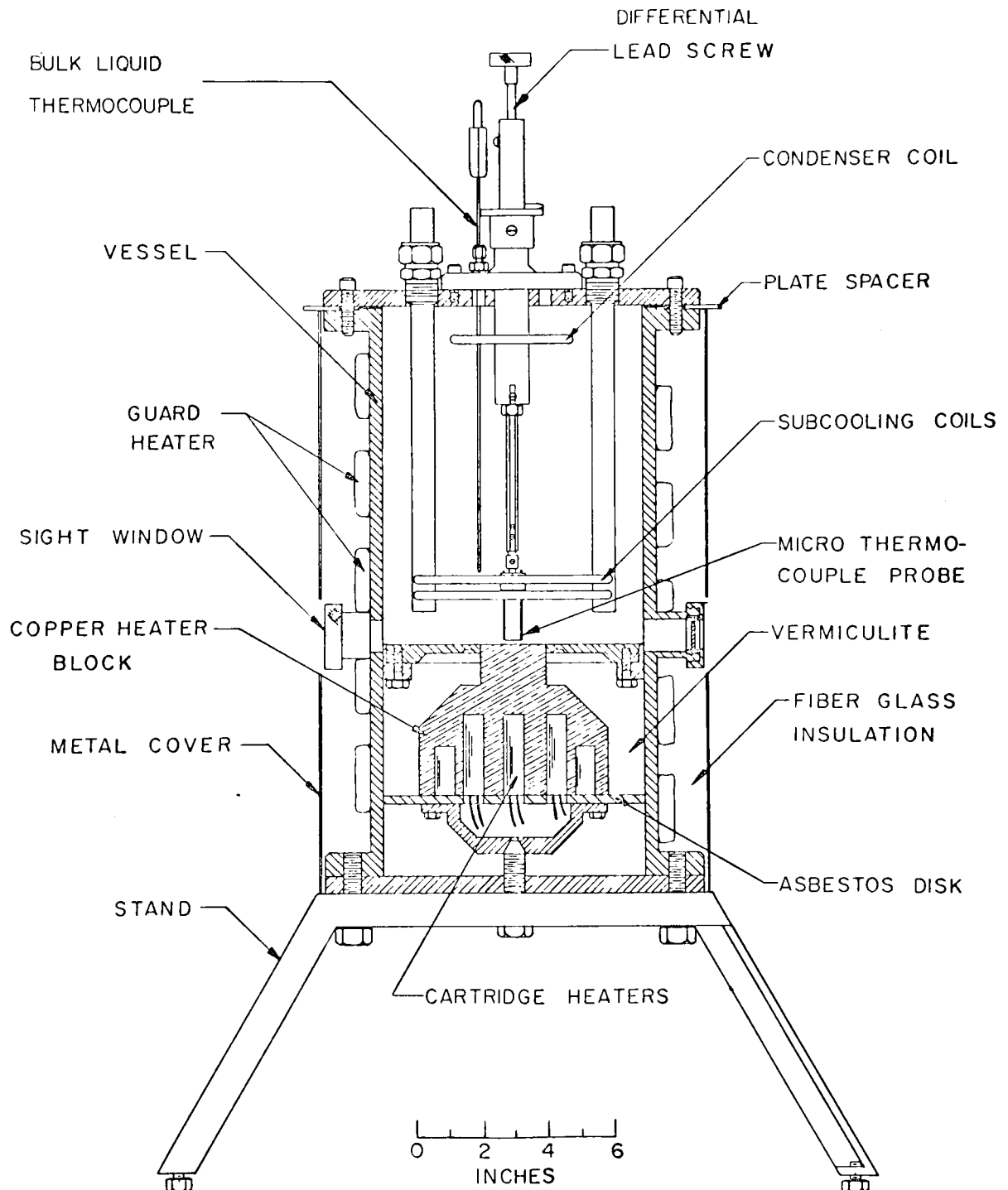


Figure 1 Section of Boiler Vessel

stainless steel cover plate was 1/2 inch thick, 11 1/2 inches in diameter and was attached to the vessel with eight 3/8 inch cap screws which compressed a rubber gasket between the cover plate and the flange. Two circular sight windows of 1 inch diameter were located diametrically opposite at a level which permitted sight parallel to and along the top of the heating surface. The heater consisted of a 6 inch copper cylinder reduced to a diameter of 2 inches at the boiling surface. Thirteen "Firerod" cartridge heaters (Watlow Electric Manufacturing Company) with a total power rating of 4000 watts were installed in symmetrically located holes in the base of the copper heater. Close contact between the cartridge heaters and the copper block was assured by reaming the holes. A stainless steel skirt with a minimum thickness of 1/8 inch was furnace welded flush with the top of the copper block to provide a continuous extension of the boiling surface. The skirt and heater assembly was held in the vessel by a mating flange welded to the inside of the vessel. Eight cap screws and an 'O' ring seal provided a water tight joint at the flange. The boiling surface was finished after the skirt was welded in place but before the heater assembly was installed in the vessel.

Initially a fine slow speed lathe cut was taken across the surface. In final finishing, number 400 'Diamond Grit' paper was first applied to the surface followed by number 600 'Diamond Grit' paper. To facilitate polishing, the heater assembly was rotated in a lathe chuck. The R.M.S. roughness of the surface was measured as approximately 5 micro inches using a Brush 'Surfindicator' model BL-110 with a hand held stylus.

To evaluate the axial temperature gradient in the copper block near the boiling surface, three chromel constantan thermocouples (thermocouples A,B, and C in Figure 2) were located on the block centreline at approximately 1/4 inch intervals from the boiling surface. The radial temperature distribution in the neck of the copper block was measured by three chromel constantan thermocouples (thermocouples D,E, and F in Figure 2) located at 1/4 inch, 1/2 inch and 3/4 inch radii from the axis in a plane perpendicular to the axis 1/2 inch below the boiling surface which included thermocouple B as well. The thermocouple assemblies were placed in 1/16 inch diameter holes drilled in the radial direction to a depth as described above. (The construction of the thermocouple assemblies is discussed in section 3.3) Two thermocouples were soldered to the underside

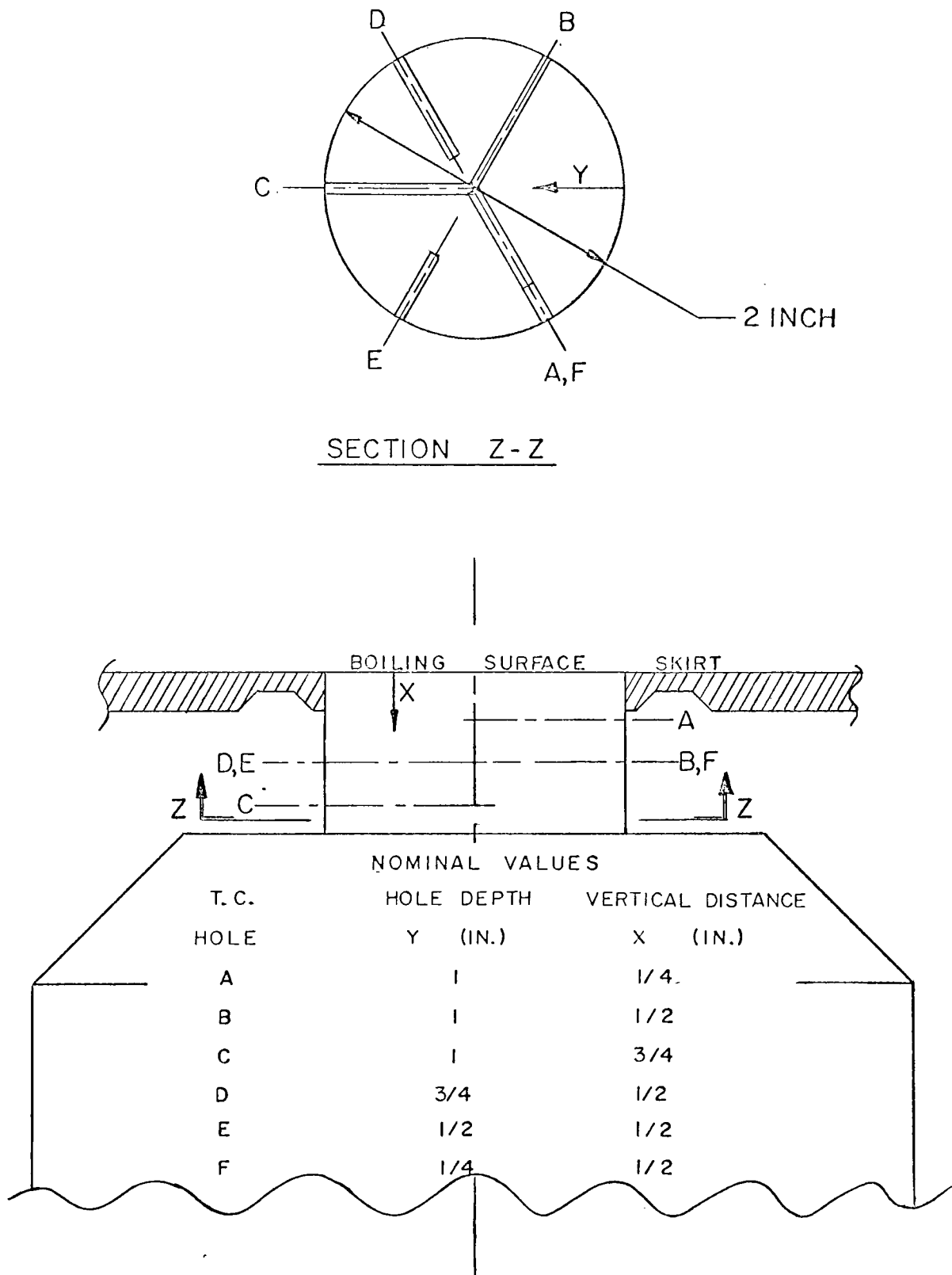


Figure 2 Location of Thermocouples in Neck of Copper Heating Block

of the skirt in 1/8 inch deep holes at 1 3/4 inch and 2 1/4 inch radii respectively. These thermocouples permitted a check on skirt temperature for various power settings. One additional thermocouple was located in the center of the cartridge heater cluster to provide a check on the maximum block temperature. In addition, two thermocouples were placed at different radii between the copper block and the vessel wall in the vermiculite insulation in order to check on radial heat loss from the copper block. The probe and traverse mechanism was mounted in the center of the cover plate. The thermocouple leads from the probe were brought through the cover plate of the vessel by a transducer gland (Conax Corporation, model TG-24-A-2-N). A description of the probe and traverse mechanism is found in section 3.4.

The present investigation required the subcooling in the bulk liquid be varied. A single pass heat exchanger of eight 3/16 inch diameter stainless steel tubes semi-circular in shape formed between two stainless steel pipes was located one inch from the skirt to provide the bulk subcooling. A single pass condenser comprised of two 3/16 inch diameter stainless steel tubes semi-circular in shape formed between two

stainless steel pipes was positioned one inch below the cover plate to condense the vapour. To satisfy a variety of cooling requirements, the two coils could be connected either in series or parallel by rubber tubing. The water flow rate through the coils was controlled by a needle valve.

As a precautionary measure the vessel was fitted with a vent to allow any non-condensed vapour to escape to the atmosphere. The vent consisted of a rubber hose attached to a 'Swaglok' fitting located on the cover plate. The vessel pressure was maintained at one atmosphere.

To minimize heat loss from the vessel outer wall, twelve feet of 3 inch wide heating tape (Electrothermal Engineering Limited, model HT 362) with a heat generation capacity of 500 watts was helically wrapped around the vessel. A 1 1/2 inch layer of fiberglass insulation covered the heating tape and an outer protective cover was formed from light gauge galvanized steel. A three legged stand of 1 inch angle iron attached to the bottom of the vessel held it upright in a stable position.

3.3. THERMOCOUPLES

Fourteen chromel constantan thermocouples were

used in the present investigation. Chromel constantan thermocouples were selected because the EMF characteristic for this combination of materials is approximately $.36 \mu \text{ volts}/^\circ\text{F}$, the maximum attainable in the temperature range under consideration. The six thermocouples installed in the neck of the copper block were constructed as shown in Figure (3). Bare 36 gauge thermocouple wire was threaded through a 1/16 inch diameter two-hole ceramic insulator. A drop of ceramic cement was used to hold the wires in place in the insulator. To achieve greater mechanical strength in the leads, 24 gauge thermocouple wire was connected to the 36 gauge thermocouple leads. The transition junction was enclosed in a 3/16 inch diameter two-hole ceramic insulator with the ends sealed with ceramic cement. A small lipped collar of brass was cemented to the small diameter insulator in such a position that when the thermocouple was fully inserted into the positioning hole, the collar was touching the outer surface of the heater neck as shown in Figure (3). Three spring loaded wires were used to hold the six thermocouple assemblies snugly in place.

Two stainless steel sheathed ceramic insulated thermocouples (Thermo Electric Company, Type 5 E0110L)

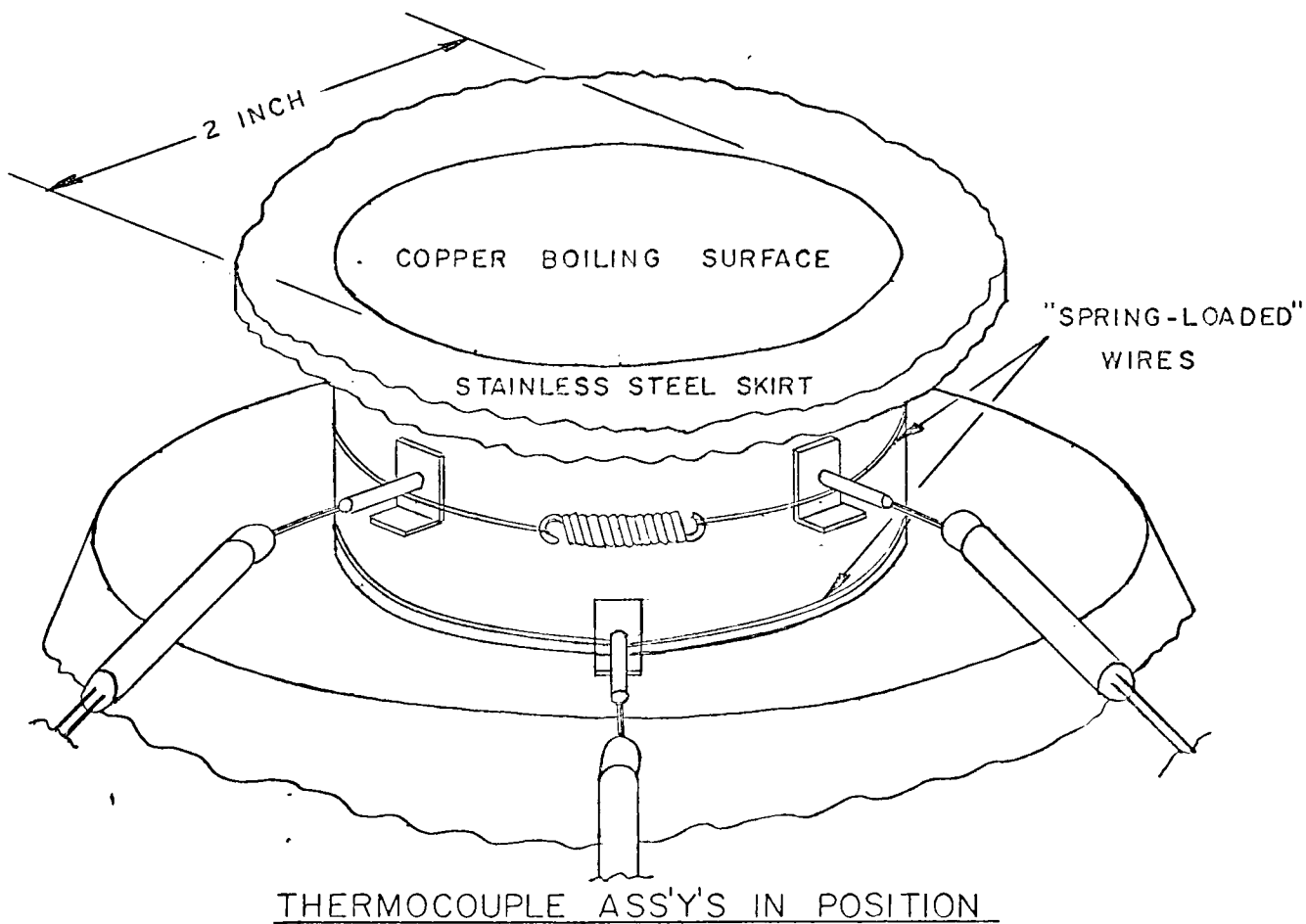
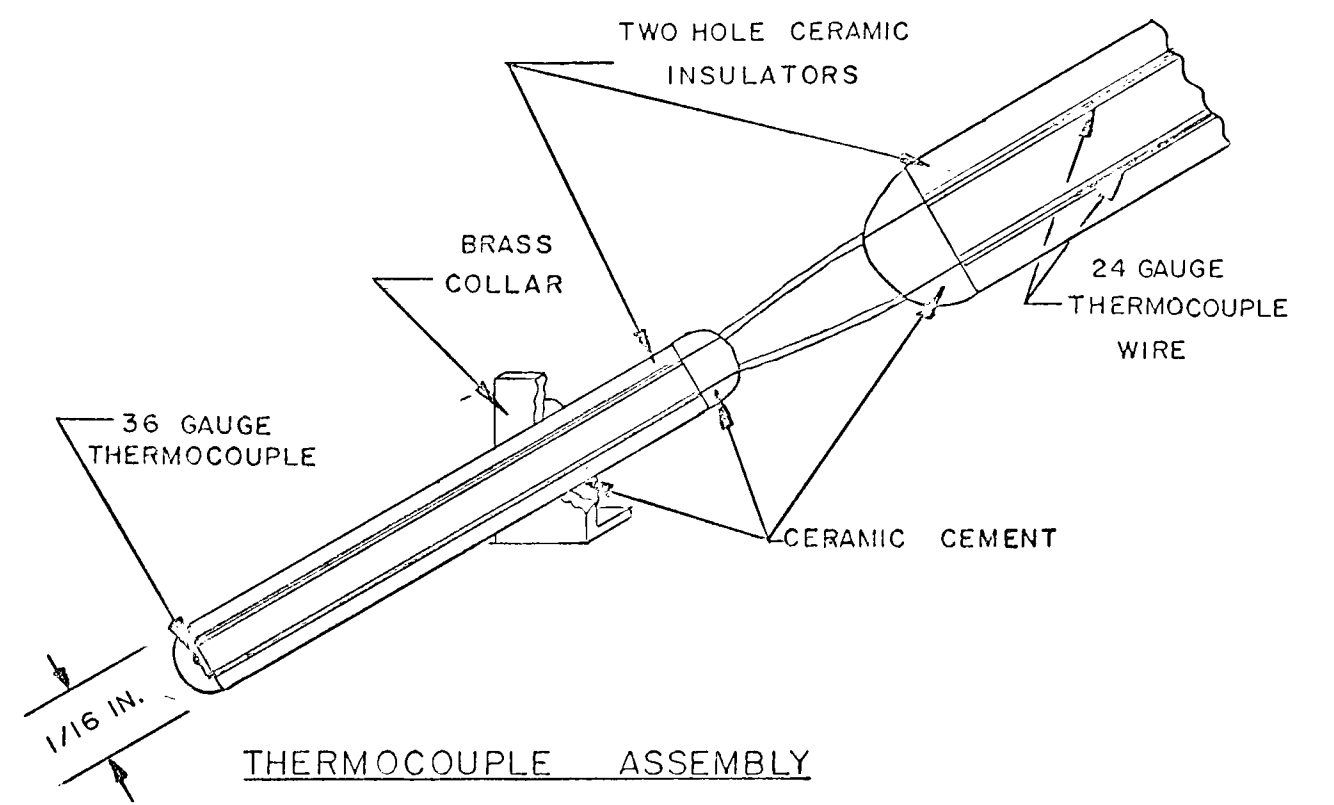


Figure 3 Thermocouple Assembly

1/16 inch in diameter were used to measure the bulk liquid temperature. Both thermocouples were introduced into the vessel through 'Swagelok' fittings in the cover plate; one at a 1 inch radius and the other at a 3 inch radius from the vessel centerline.

All the thermocouples were standardized by placing them in a constant temperature environment and comparing their reading with that of a mercury in glass thermometer. In all cases the deviation in temperature reading was less than 1°F.

3.4. THERMOCOUPLE PROBE AND TRAVERSE MECHANISM

The single most important component of the entire apparatus was the thermocouple probe and traverse mechanism. The purpose of the probe was to traverse the boundary layer in the immediate vicinity of the heating surface and to measure the fluctuating temperature within it. Previous investigators (Marcus and Dropkin, Lippert and Dougall, Judd) found the temperature gradient to be extremely steep; approximately 4000 °F/inch in some cases. Consequently, it was essential that the thermocouple probe be capable of measuring extremely localized temperatures and that the position of the probe be known within 0.001 inch.

Figure (4) is an illustration of the thermocouple probe and traversing mechanism. The primary feature of the traversing mechanism is a differential lead screw, the operation of which is dependent upon the relative motion of two components in response to rotation of a single threaded shaft with different threads on each end. The input end of the differential lead screw shaft was threaded with $1/4 - 28$ UNF thread into the fixed portion of the differential lead screw which in turn was fixed to the cover plate of the vessel; one rotation moved the shaft $1/28$ inch relative to the cover plate. The output end of the differential lead screw shaft was threaded with $3/8 - 32$ UNEF thread into the moving portion of the differential lead screw onto which the probe was attached; one rotation moved the probe $1/32$ inch relative to the shaft since the rotation of the moving portion was prevented by a small set screw. Consequently, the differential motion was simply the difference between $1/28$ inch and $1/32$ inch which is equivalent to $1/224$ inch per revolution of the shaft.

To assure smooth operation, the lead screw shaft was constructed of brass while the other components were made of stainless steel. To compensate for imperfection in the threads characterized by backlash, a compression spring was placed between the moving portion of the lead screw and the fixed portion. In this manner any backlash was always in the same direction

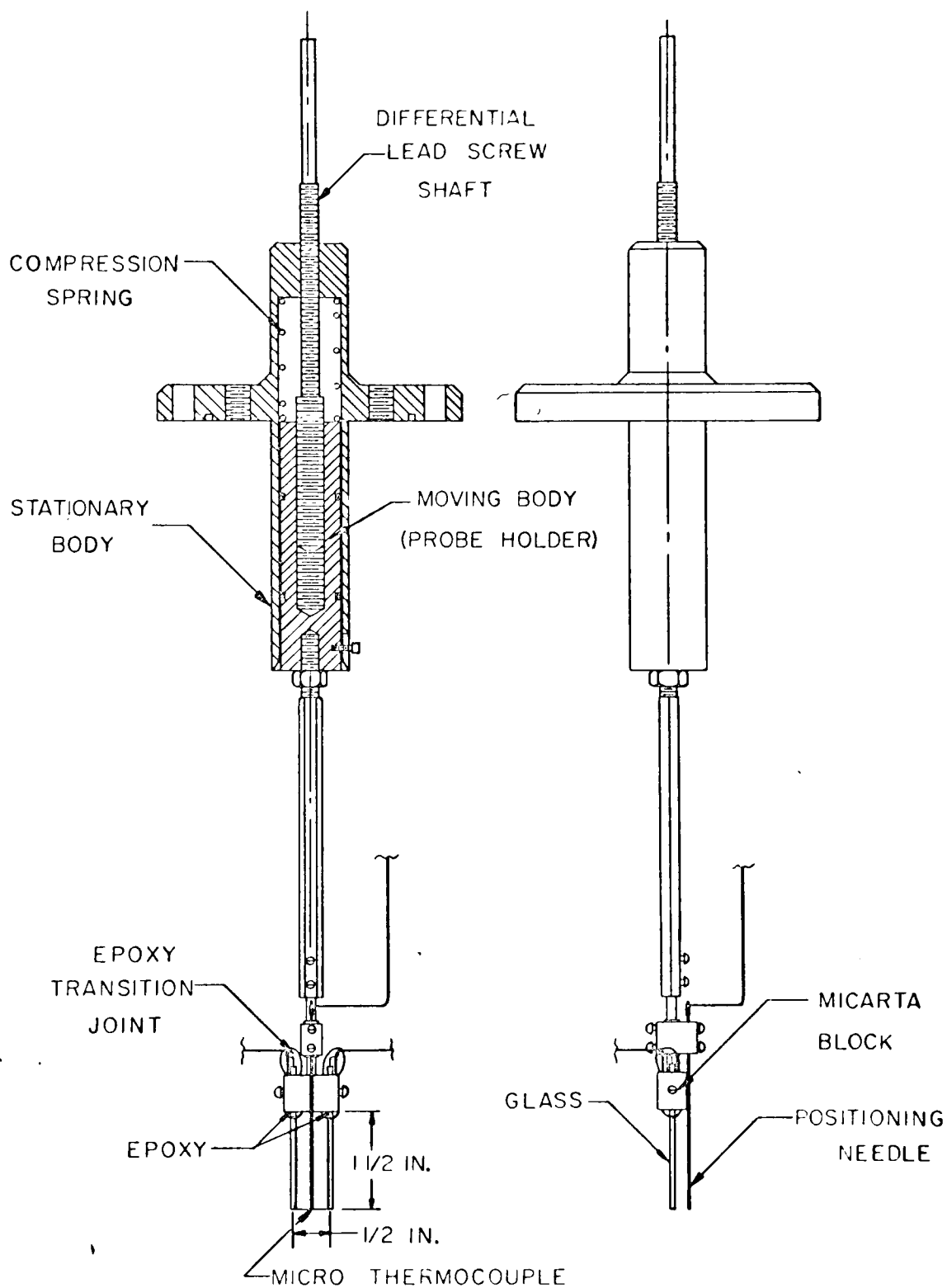


Figure 4 Micro-Thermocouple and Traverse Mechanism

and did not appear in probe position uncertainty. Two 'O' rings were set into the moving portion of the lead screw to assure the probe remained concentric and to act as a pressure seal. The lead screw was turned manually. Revolution counting was aided by a pointer attached to the input shaft and a fixed dial.

The techniques of Gelb, Marcus and Dropkin (8) were applied to the design and construction of the thermocouple probe. In the manufacture of the thermocouple itself, bare chromel and constantan wires 0.001 inch in diameter were joined by discharge welding. Experience showed that with care the diameter of the thermocouple bead could be held below 0.003 inches. The thermocouple support was constructed of two 1/16 inch diameter glass capillary tubes held 1/2 inch apart by a micarta block. Heat loss considerations made it desirable for the thermocouple leads suspended between the supports to be in an isothermal plane. As measurements indicated that the boiling surface and the top flange were not parallel, it was necessary to locate the glass thermocouple supports with the cover plate and traversing assembly in place on the vessel. By trial and error the lower ends of the supports were positioned equidistant from the boiling surface. The location of the two supports relative to the boiling

surface could be determined within 0.0015 inches by sighting a precision optical level through the sight window. Epoxy and two set screws fixed the position of the supports in the micarta block. To assure that the two glass supports would maintain the same position relative to the surface after each reassembly, two precautions were taken. Four aluminum spacers (Figure (1)) of less thickness than the rubber gasket were symmetrically placed between the cover plate and the flange. The gasket was compressed to provide a seal but the relative axial and rotational position of the cover plate to the flange remained the same after each reassembly. The fine wire thermocouple leads were threaded through the capillary tubes and weights were attached to the leads with the probe assembly held inverted. With the weights providing tension in the thermocouple wire, the glass supports were slightly sprung inward. While in this loaded condition epoxy was applied to the lower end of the capillary tubes. Thus with the hardened epoxy holding the fine wire in place, the sprung capillary tubes provided tension over the span of 0.001 inch wire. As a consequence, vibration in the span of fine wire was kept to a minimum. As the 0.001 inch thermocouple wire had low mechanical

strength, a transition was made to 24 gauge thermocouple wire in the immediate vicinity of the micarta block. The entire junction was surrounded and anchored to the micarta block by epoxy. This proved to be a successful way in which to prevent breakage of the fine wire thermocouple leads.

In making a traverse of the thermal boundary layer it was important to know the position of the probe thermocouple above the heated surface. It was initially planned to have the thermocouple bead touch down on the surface and make electrical contact, thus indicating its position. It was found that the oxide which had formed on the copper heating surface prevented electrical contact. To overcome this difficulty a needle was mounted on the probe holder which could penetrate the thin oxide and make electrical contact with the surface. By knowing the position of the thermocouple bead relative to the needle tip, the probe position could be determined with respect to the surface. A precision optical level was used to determine the vertical distance between the thermocouple bead and the tip of the needle which in all cases did not exceed 0.004 inch. The lead to the needle was introduced into the vessel through a transducer gland in the cover plate.

3.5. POWER CIRCUITRY AND MEASUREMENT

A power circuit diagram for the apparatus is shown in Figure (5). The line voltage was fed directly into a 230 volt 4.2 KVA 'Powerstat' variable output autotransformer which controlled the power input to the thirteen 'Firerod' resistance heaters. A wattmeter was used to measure the power dissipated in the heaters which were connected in parallel at a covered barrier strip. A 120 volt 1.4 KVA 'Powerstat' variable output autotransformer controlled the power to the guard heaters and another wattmeter measured the power drawn by them.

3.6. TEMPERATURE MEASURING SYSTEM

A typical thermocouple circuit is shown in Figure (6). To conserve chromel constantan lead wire a transition was made to single strain nylon insulated thermocouple grade copper wire at an ice bath in all of the thermocouple circuits. The thirteen pairs of leads were then connected to a switch board on which double pole, double throw copper knife switches directed the desired output signal to the type 9160G Guildline potentiometer capable of reading with an accuracy of $1 \mu \text{ volt} \pm 0.0005\%$ of the reading. The copper leads were shielded by a covering of aluminum

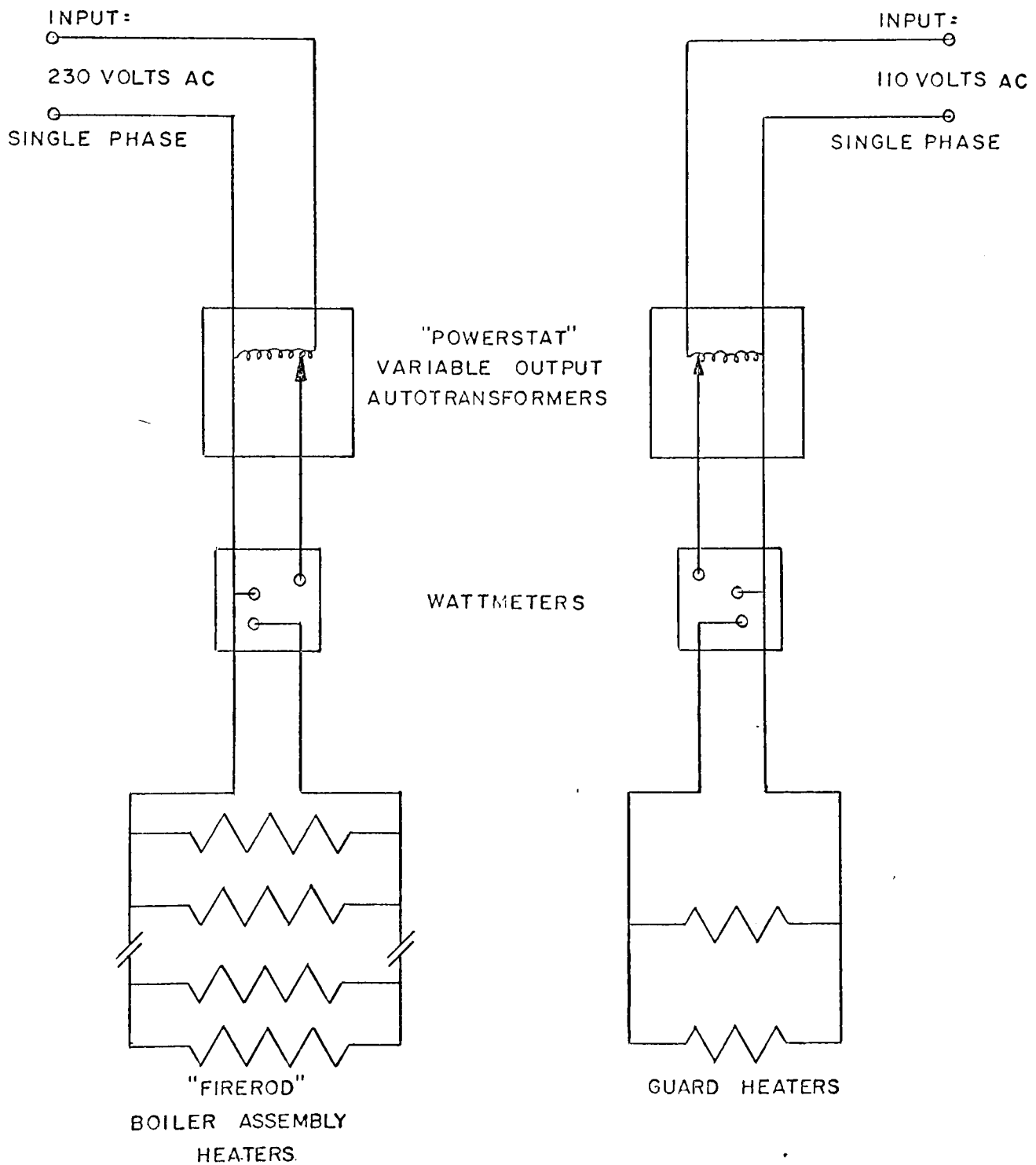


Figure 5 Power Circuit Diagram

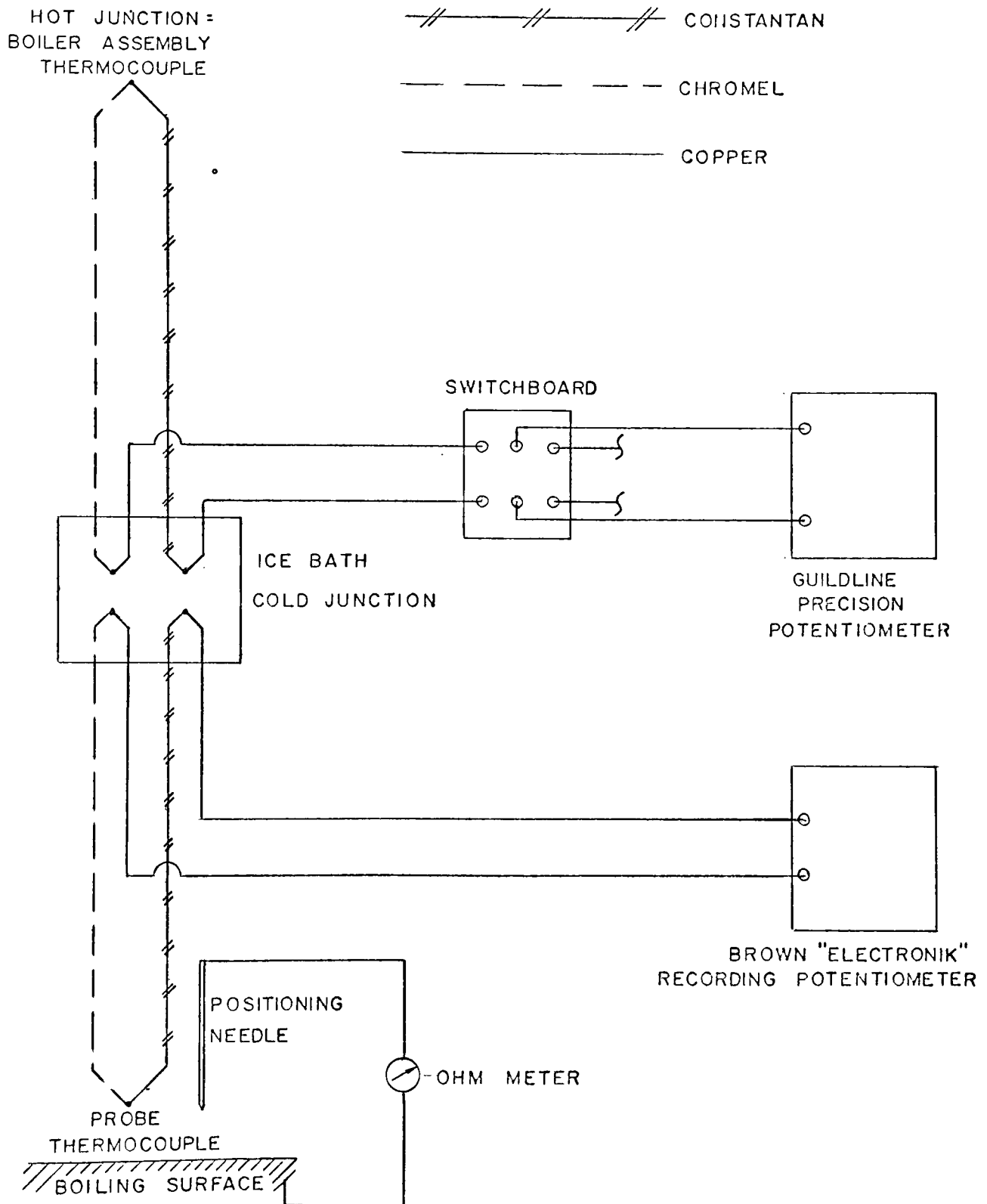


Figure 6 Thermocouple Circuit Diagram

foil grounded to a water pipe. The signal from the probe thermocouple was fed directly to a Brown 'Elektronik' (model Sy 153 x 18 -(V AH 1) -11-111-157-D) single pen continuous recording potentiometer that had an accuracy capability of $\pm 0.25\%$. Provision was made to allow the continuous recording of the bulk liquid temperature on the recording potentiometer when a probe traverse was not in progress. With the exception of the probe thermocouple, all temperature measurements were made on the Guildline potentiometer. In general the span on the recording potentiometer was set at 10 millivolts. The chart speed was set at 18 inches/minute when recording boundary layer traverse data.

4.

TEST CONDITIONS

The investigation was subdivided into two series of tests; one in which the subcooling was varied at a given heat flux, the other in which incipience of boiling was achieved at a number of subcooling conditions. The three heat flux settings for the first series of tests were selected to explore three boiling regimes as described by Gaertner (9); the discrete bubble region (20,000 BTU/HRFT²), the first transition region (50,000 BTU/HRFT²) and the vapour mushroom region (100,000 BTU/HRFT²). The maximum level of subcooling in each test was limited by the design of the subcooling coil. Two intermediate levels of subcooling between the maximum and minimum obtainable values were selected so as to divide the subcooling range into three approximately equal steps.

A series of tests were performed to determine the incipience of boiling for five levels of subcooling.

Table I shows the nominal values of heat flux and subcooling for the two series in tabular form.

TABLE I
NOMINAL VALUES
SATURATED AND SUBCOOLED BOILING TESTS

Test No.	Q/A BTU/HRFT ²	Subcooling °F
1 A	20,000	0
B	20,000	15
C	20,000	40
D	20,000	52
2 A	50,000	0
B	50,000	33
C	50,000	67
D	50,000	105
3 A	100,000	0
B	100,000	32
C	100,000	58
D	100,000	89
<u>INCIPIENCE OF BOILING TESTS</u>		
4	3,400	10
5	5,000	24
6	8,400	21
7	14,400	32
8	40,000	112

5.

TEST PROCEDURE

At the beginning of each test while the vessel was 'cold' the location of the tip of the positioning needle relative to the thermocouple bead was measured with the precision optical level. This gave the position of the thermocouple bead with respect to the heating surface when the needle made electrical contact with the surface. The probe assembly was then lowered until the needle came in contact with the boiling surface after which it was raised a given number of turns of the differential lead screw shaft, in most cases 15 turns. The vessel was filled with approximately 6 inches of deionized distilled water and the guard heaters and copper block heaters were turned on. A heater power setting corresponding to the highest heat flux of any test, approximately $100,000 \text{ BTU/HRFT}^2$ was used to heat up the boiler assembly quickly. The heat up time was approximately 1 to 1 1/2 hours. To assure that the nucleation sites were properly activated at the beginning of each test, saturated boiling at the $100,000 \text{ BTU/HRFT}^2$ setting was allowed to continue for twenty minutes after which the power was reduced to the desired level for the test. In all the tests the guard heaters had a power input of 125 watts.

Depending on the level of heat flux, 1 1/2 to 2 hours were required for the system to regain thermal equilibrium after a change in heat flux or subcooling took place. For the tests in which probe traverses at four levels of subcooling were required, the first traverse was taken with the water boiling under saturated conditions. Following this, the maximum subcooling condition was achieved after which the two subsequent lower subcooling conditions were established. The test was ended by allowing the system to regain the saturated boiling condition.

All thermocouples were read on the Guildline Potentiometer immediately before and after each probe traverse to provide a check on the temperature stability. The barometric pressure reading was recorded at the end of each traverse.

Twenty to thirty minutes were required to make a complete traverse of the thermal boundary layer. In general, the probe was lowered from its maximum height in increments of one revolution of the lead screw shaft. When the probe reached a level of approximately 0.015 inches above the boiling surface, the increments were decreased to 1/2 or 1/4 turns depending on the severity of the temperature gradient in the liquid.

At each probe position the temperature fluctuations were recorded on the Brown 'Elektronik' recording potentiometer for approximately one minute. The position of the probe (in turns of lead screw shaft) was recorded on the chart paper for each segment of the traverse. A continuous recording of the bulk temperature was made on the recording potentiometer in between probe traverses which aided the regulation of the level of subcooling in the bulk liquid.

During the tests of the incipience of boiling, observation was made of the appearance of the first bubble. The heat flux and subcooling were noted and a complete traverse was performed in the manner described above.

6.

DATA REDUCTION

The evaluation of heat flux from the boiling heat transfer surface is given by:

$$\left(\frac{Q}{A}\right)_{\text{ACTUAL}} = \left(\frac{Q}{A}\right)_{\text{INPUT}} - \left(\frac{Q}{A}\right)_{\text{LOSS}} \quad (6)$$

In Equation (6), $(Q/A)_{\text{ACTUAL}}$ is the heat flux from the boiling surface, $(Q/A)_{\text{INPUT}}$ is the apparent heat flux derived from the electrical power supplied to the heater assembly and $(Q/A)_{\text{LOSS}}$ is the portion of $(Q/A)_{\text{INPUT}}$ that does not appear at the boiling surface and is lost to the surroundings through the stainless steel skirt from the bottom of the heater assembly and through the vermiculite. The maximum percentage heat loss was approximately 50% in the lowest heat flux tests. Appendix A presents an extensive treatment of the heat loss evaluation.

The surface superheat, θ_w , is given by

$$\theta_w = T_w - T_{\text{sat}} \quad (7)$$

where T_{sat} is the saturation temperature corresponding to the total pressure at the boiling surface comprised of the barometric pressure and the hydrostatic pressure, and T_w is the temperature of the boiling surface obtained by extrapolating the temperature gradient in the neck of the heater block to the boiling surface.

Appendix B describes a test performed to investigate the extrapolation procedure.

The bulk liquid subcooling, θ_{sub} , is given by

$$\theta_{sub} = T_{sat} - T_b \quad (8)$$

where T_{sat} is the saturation temperature defined above and T_b is the temperature of the bulk liquid measured 2 inches above the boiling surface. Appendix C reports a test which demonstrates that the location chosen to measure bulk liquid temperature is sufficiently removed from the boiling surface that the liquid temperature is invariant with axial and radial position.

The position of the probe with respect to the boiling surface was determined by

$$Z = Z_0 + N(0.00445) \quad (9)$$

In this relationship Z is the vertical distance from the boiling surface to the centerline of the probe thermocouple, Z_0 is the vertical distance between the tip of the positioning needle and the centerline of the probe thermocouple, and N is the number of turns of the differential lead screw shaft which the positioning needle has been moved from contact with the boiling surface. The constant in Equation (9) arises because

one turn of the differential lead screw shaft gives the probe a linear movement of 0.00445 inches.

The frequency and amplitude of the probe thermocouple signal made it difficult to determine a mean value for a given probe setting. This observation was most evident in the case of highest bulk subcooling. A planimeter was used to determine the area under a representative length of trace (6 to 8 inches) and thus an average value could be calculated. In general, a planimeter traverse was taken twice over a given area to assure reproducibility in the planimeter reading.

The physical and thermophysical properties required in the calculations were taken from "Thermodynamic Properties of Steam" by Keenan and Keyes, the ASME handbook "Metal Properties", and the "ASHRAE Guide and Data Book".

In this section, the experimental data is presented without comment. A discussion on the data is presented in Section 8. The experimental and calculated data is tabulated in Appendix E.

Figure (7) shows a plot of heat flux Q/Λ as a function of superheat θ_w and compares the results of this investigation with those of Gaertner and Lippert and Dougdall. Figure (8) is a plot of wall superheat and bulk liquid subcooling for test series 1, 2 and 3. Figures (9), (10) and (11) are plots of the temperature profiles taken in the test series 1, 2 and 3 while Figure (12) is a similar plot for the incipience of boiling tests.

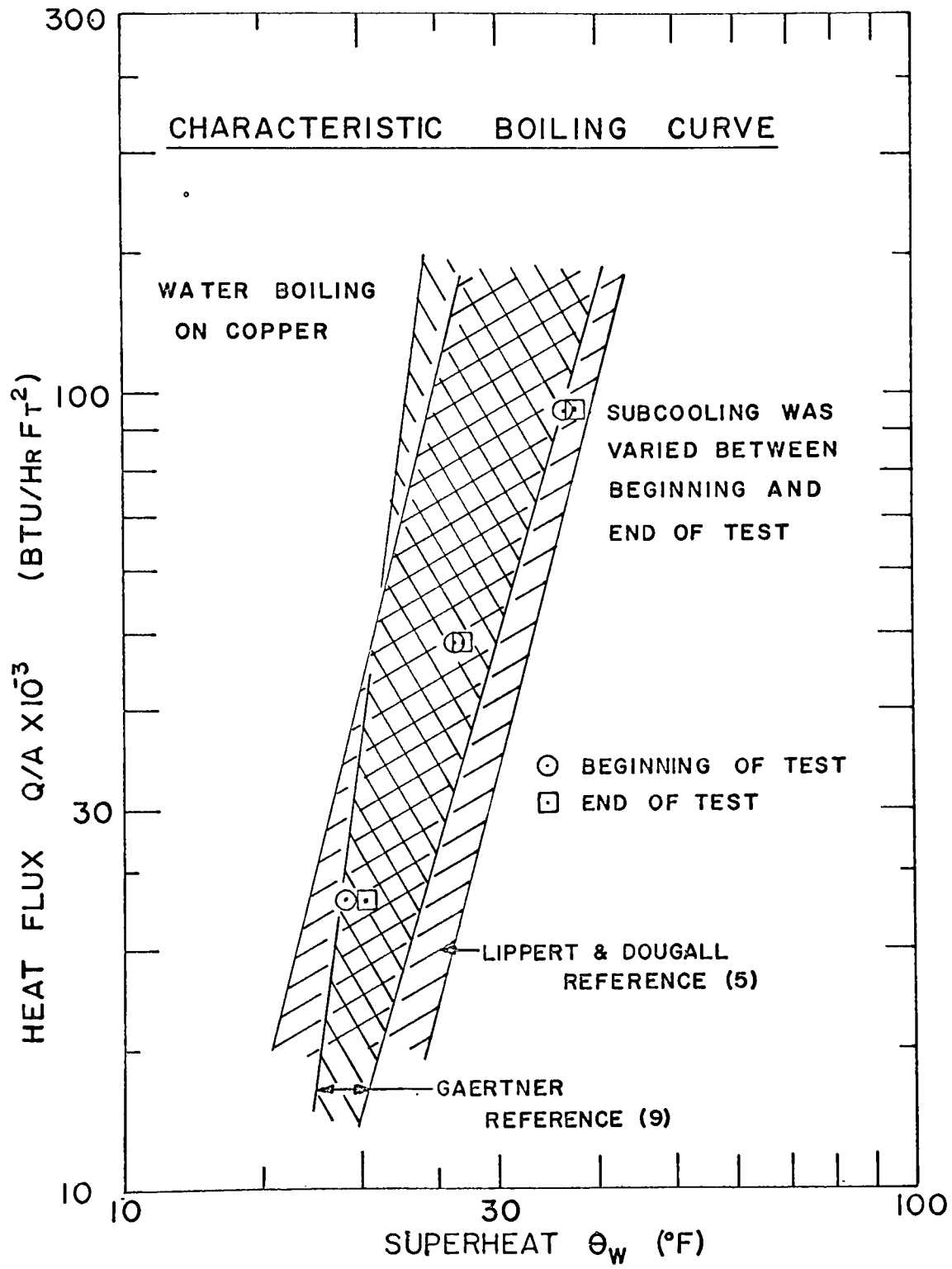


Figure 7 Characteristic Boiling Curve

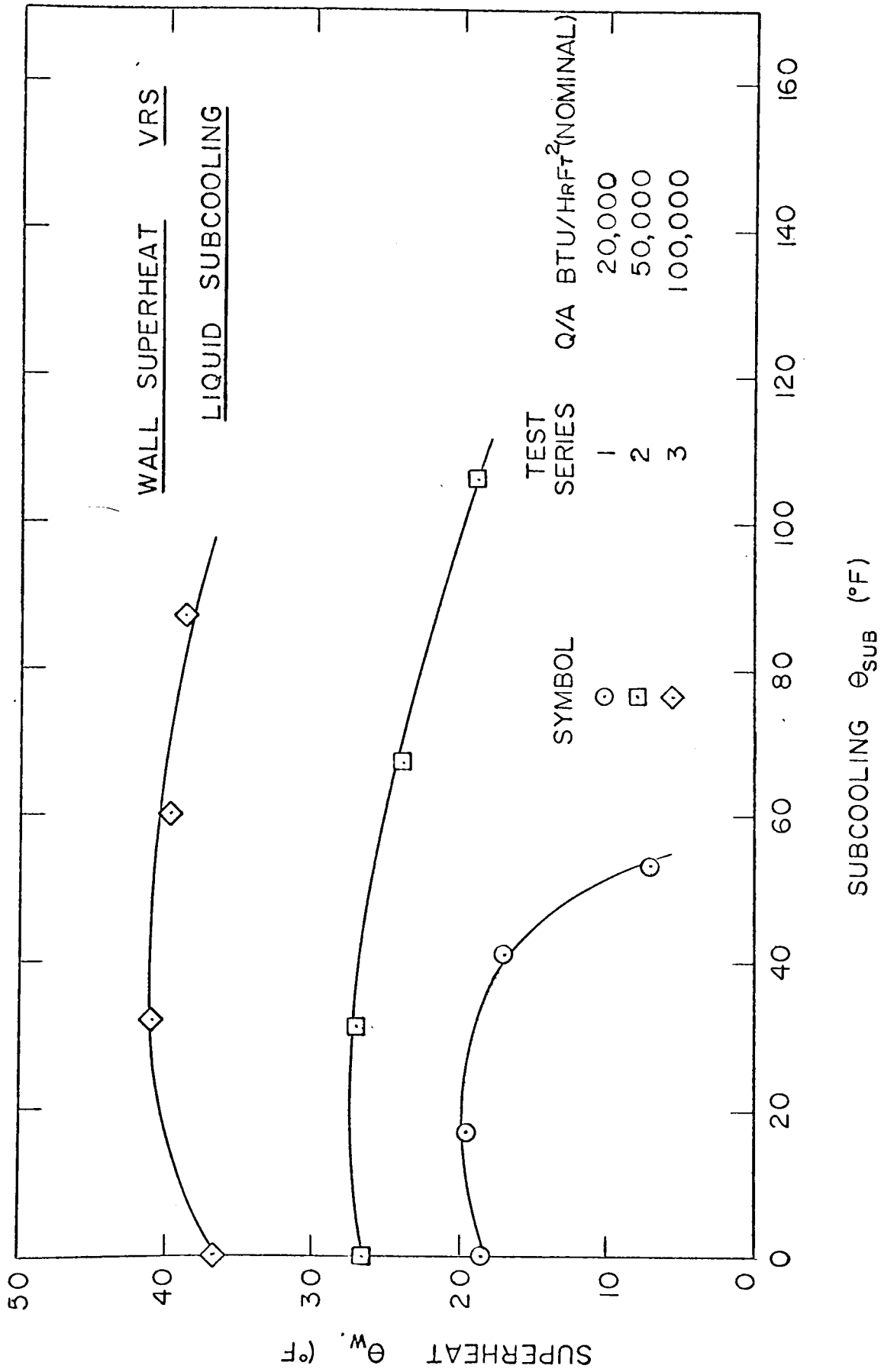


Figure 8 Variation of Wall Superheat with Bulk Subcooling

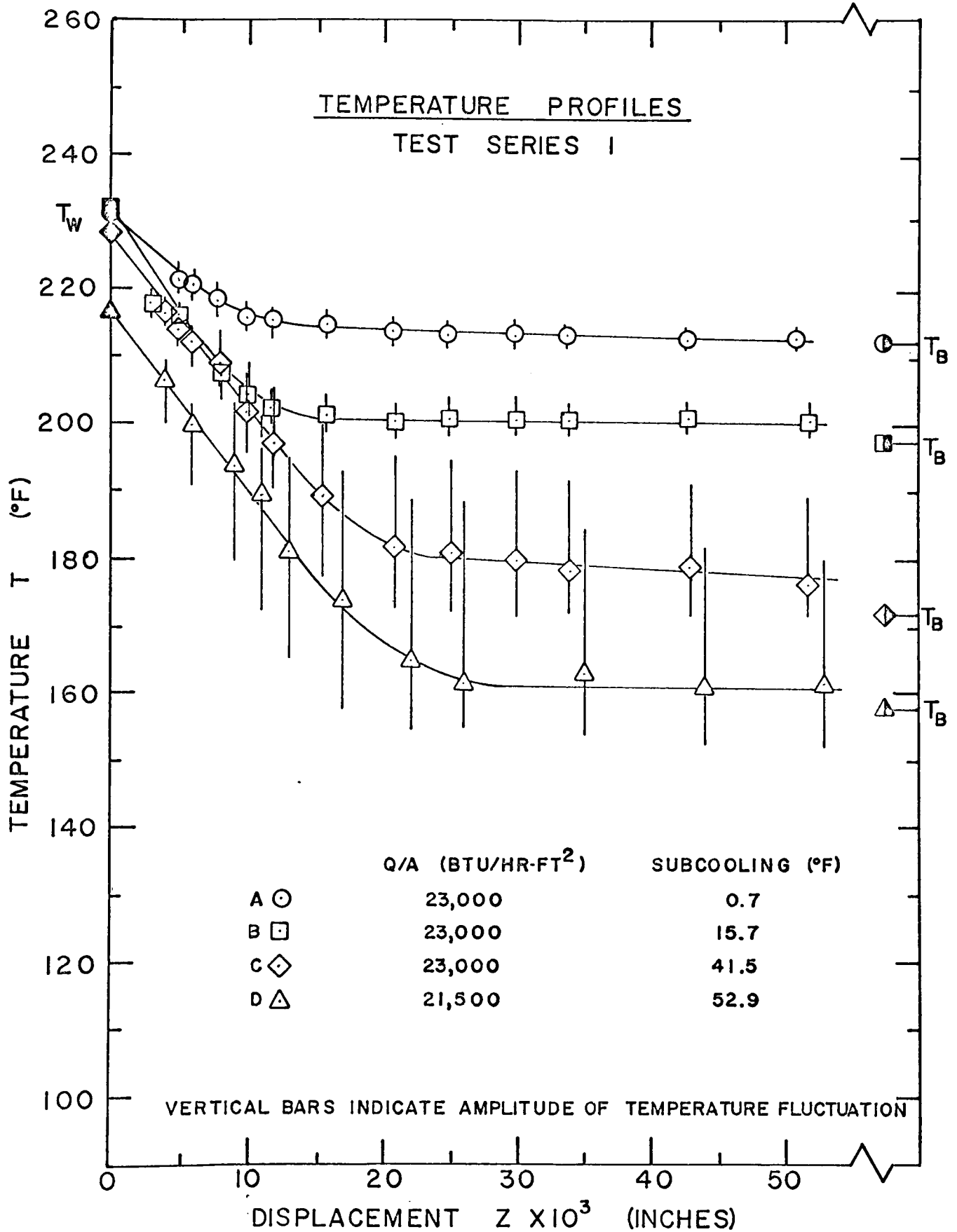


Figure 9 Temperature Profiles at $Q/A = 20,000$ BTU/HRFT²

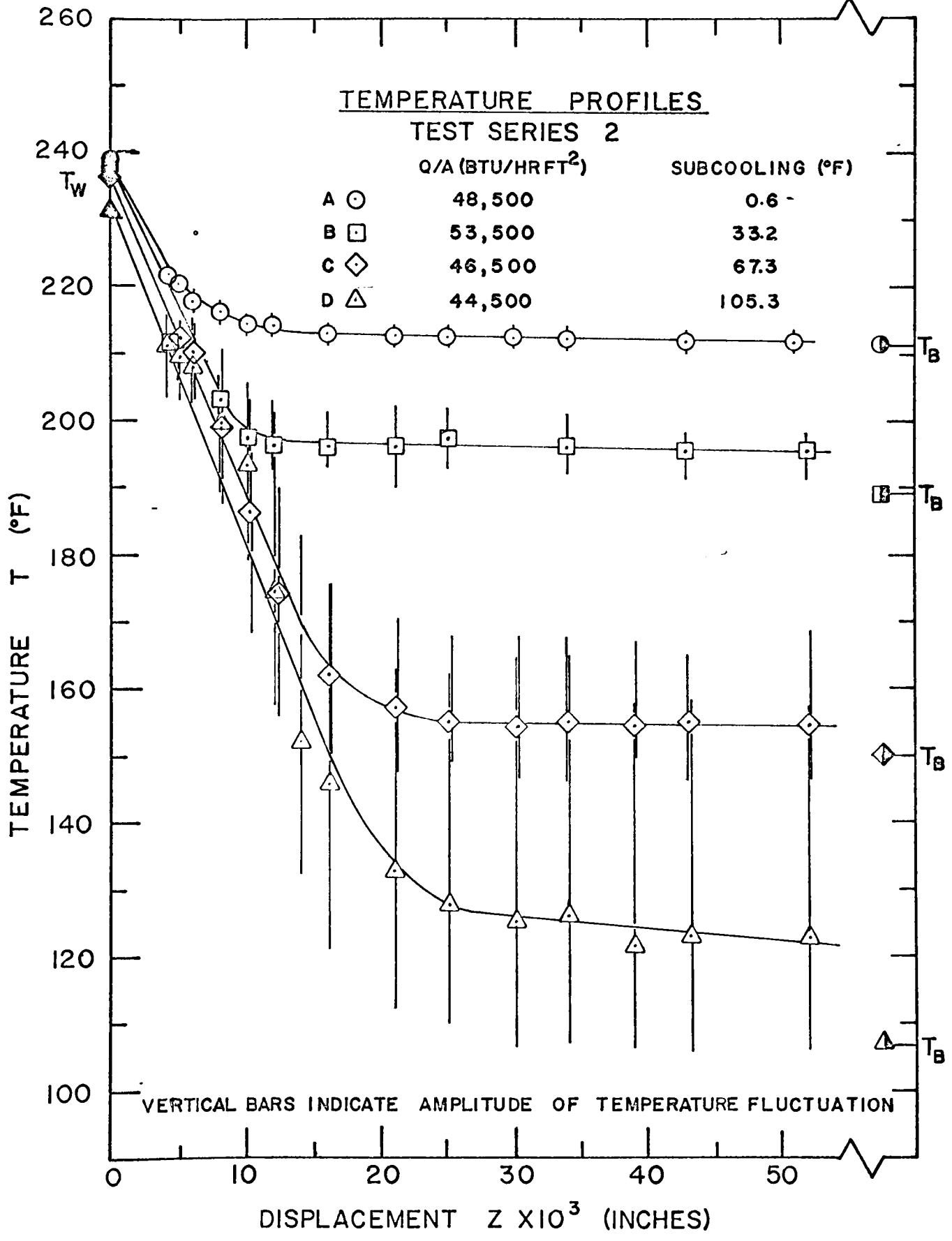


Figure 10 Temperature Profiles at Q/A = 50,000 BTU/HRFT²

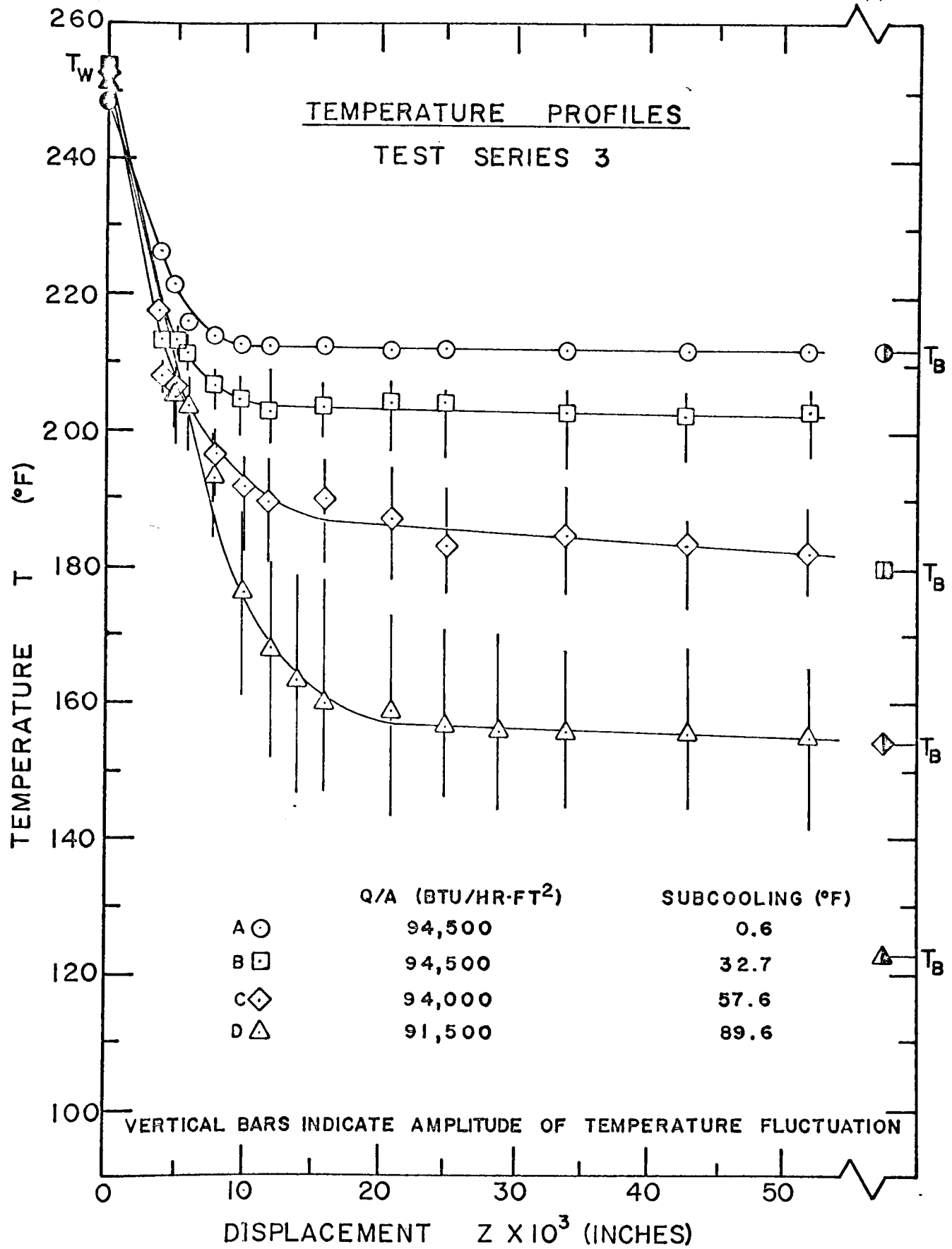


Figure 11 Temperature Profiles at Q/A = 100,000 BTU/HRFT²

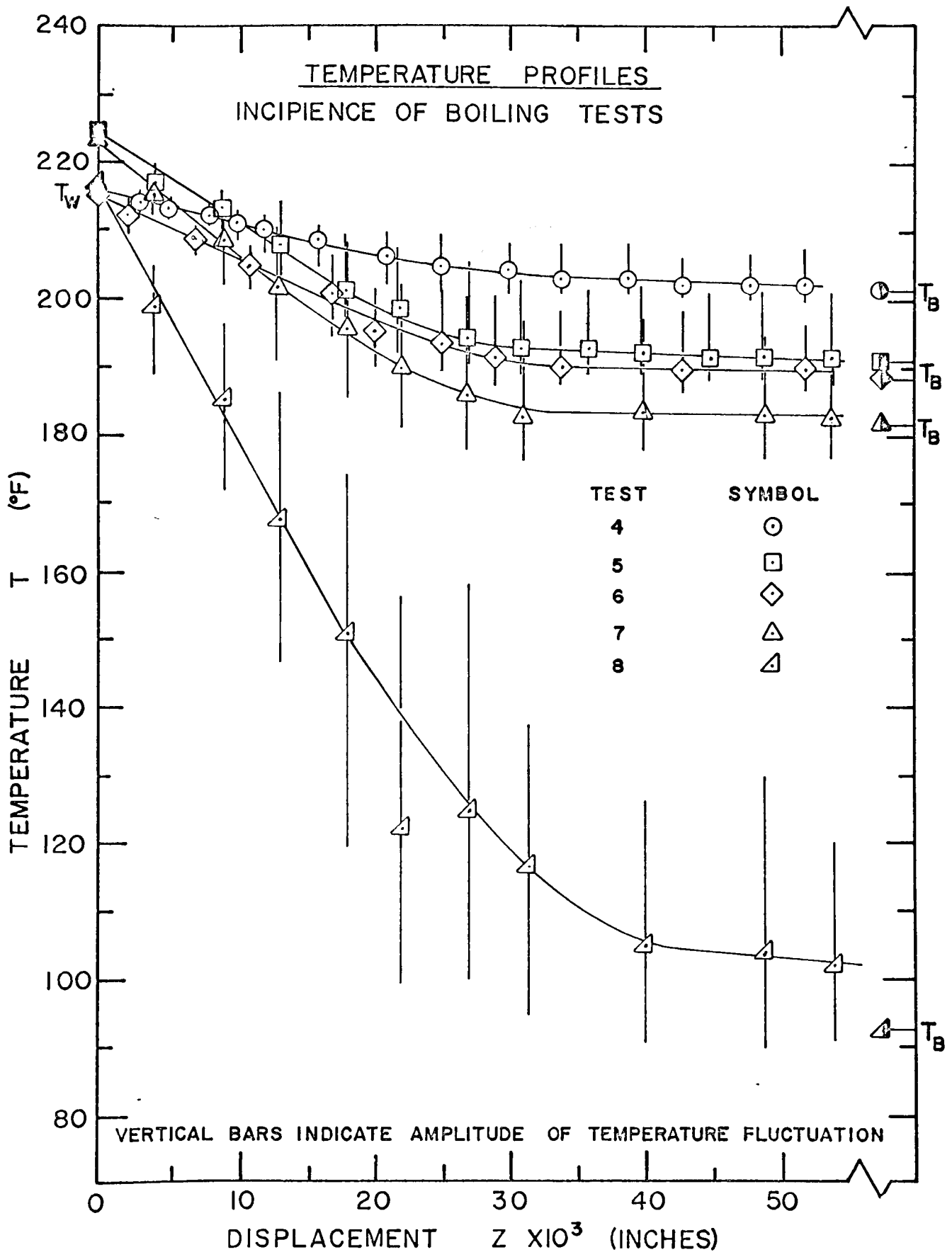


Figure 12 Temperature Profiles at Incipience of Boiling Condition

Figure (7) is a plot of wall superheat (θ_w) versus heat flux (Q/A). The two data points at each of the test heat fluxes were taken at the beginning and end of the test. The two points for each of the test heat fluxes are nearly coincident, which is an indication that the surface condition did not change appreciably by a sequence of changes in subcooling. It may be concluded that the active site density, bubble emission frequency and bubble size were the same at the beginning and end of the individual tests. The experimental data falls well within the range of data reported by previous investigators, Lippert and Dougall (5) and Gaertner (9) who have also boiled water on copper surfaces. Thus, some confidence is established in the present work. The effect of varying subcooling at constant heat flux is shown in Figure (8).

All the measured temperature profiles in the liquid adjacent to the boiling surface appear to be characterized by a linear portion immediately above the boiling surface as seen in Figures (9), (10), (11) and (12). This feature is most readily seen in the profiles taken at the incipience of boiling where the temperature gradient in the liquid near the surface has the lowest

value. Marcus and Dropkin (4) and Lippert and Dougall (5) have determined that the linear portion of the temperature profile extends to the surface. On this basis, the measured profiles have also been extended to the surface temperature value determined from an extrapolation of the axial temperature gradient in the neck of the heating block. An example of the uncertainty in measuring the temperature profiles given by an uncertainty analysis presented in Appendix F is seen in Figure (13).

A significant observation to be made from the temperature profiles is that the amplitude of the temperature fluctuations appear to reach a maximum at approximately the same distance from the surface that the mean temperature variation deviates from the bulk temperature. The temperature fluctuations decrease to a minimum near the surface indicating the surface acts as a "smoothing agent" inhibiting agitation of the liquid.

It is important to define the "thermal boundary layer thickness" since the present study was undertaken to investigate the variation of this parameter with heat flux and subcooling. Yamagata (10) et al has defined the thermal layer thickness, ξ , as the height above the surface beyond which the average bulk liquid temperature is uniform. Referring to Figure (13) one sees that it

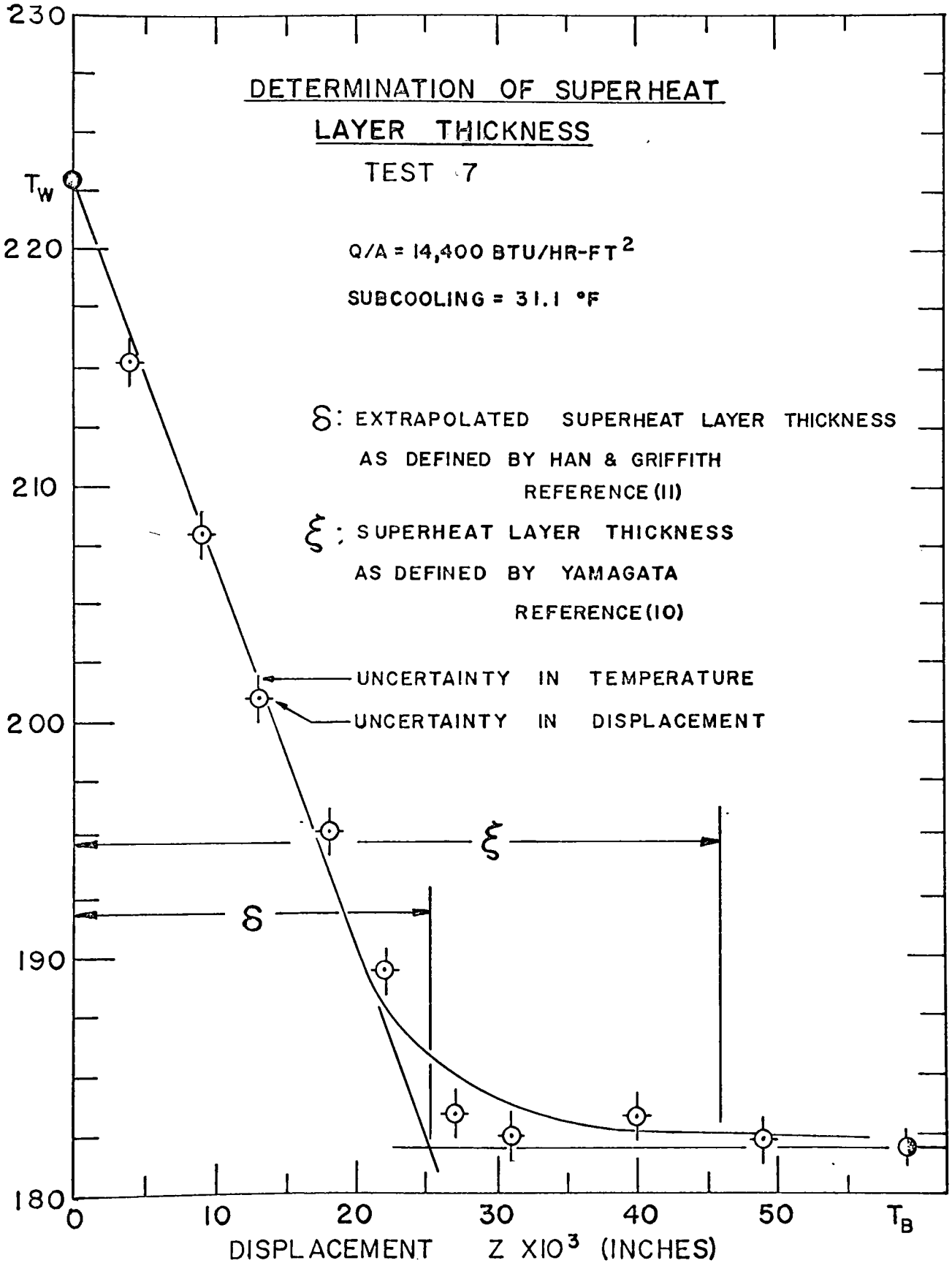


Figure. 13 Determination of Superheat Layer Thickness

is difficult to say at exactly what height this condition is attained. The region of high liquid superheat extends only a few hundredths of an inch from the surface which is considerably smaller than the thickness ξ as defined by Yamagata. The region of high liquid superheat probably influences nucleation and bubble dynamics to a large degree and hence it is felt that Yamagata's definition does not sufficiently reflect the importance of the boundary layer.

Han and Griffith (11) have defined a more representative value for boundary layer thickness. Assuming that the temperature distribution closest to the surface is of greatest importance, a thickness δ can be defined as the height of the intersection between the tangent to the temperature profile at the surface and the constant liquid bulk temperature line as shown in Figure (13). The tangent line which defines δ is actually an extrapolation of the linear portion of the temperature distribution to the bulk liquid temperature. Hence, the parameter δ is called the "extrapolated superheat-layer thickness". It is felt that this definition of boundary layer thickness closely reflects the thickness of the superheat region of the thermal boundary layer and consequently δ was used in the

following analysis.

As reported in 'References (3-6)' the present work indicates that the extrapolated superheat-layer thickness is a function of heat flux. Tests 1A,2A and 3A (Figures (9),(10) and (11)) for boiling under saturated conditions indicate that δ decreases with an increase in heat flux. For a four fold increase in heat flux, δ decreases by approximately one half. The influence of increased levels of subcooling on δ is noticed to have a reverse effect. In tests 1, 2 and 3 for a fixed heat flux, a pronounced increase in δ occurs with each increase in the level of subcooling. Both of these trends are thought to be a direct result of the degree of turbulence in the bulk liquid. In the constant subcooling case, an increase in heat flux results in more vigorous boiling. More bubbles are emitted from the surface per unit area per unit time causing greater mixing resulting in the establishment of a thinner δ . The effect of varying the level of subcooling can be explained in a similar manner. It was observed that in the case of boiling with a highly subcooled bulk liquid, fewer smaller bubbles left the boiling surface per unit time per unit area than in the case of saturated boiling. The characteristic mode of heat transfer had changed

from nucleate boiling to natural convection. It is reasonable to assume then that by suppressing bubble growth and departure with bulk subcooling, the bulk turbulence and mixing is also suppressed resulting in the establishment of a thicker δ .

The present investigation undertook to study the incipience of boiling as well. Figure (14) presents the results of these tests. Equation (5) which is reproduced below for convenience

$$\theta_{wo} = \theta_{sub} + \frac{2AC_3}{\delta} + \left[\left(2\theta_{sub} + \frac{2AC_3}{\delta} \right) \left(\frac{2AC_3}{\delta} \right) \right]^{1/2} \quad (5)$$

was used to predict the incipient boiling wall superheat, θ_{wo} by substitution of experimentally determined values of δ and θ_{sub} . Figure (14) is a comparison of the experimental values of θ_{wo} and θ_{wo} predicted by Equation (5). In general, the agreement between the experimental and predicted values of θ_{wo} is good and indicates the validity of Hsu's mathematical model for nucleation.

Marcus and Dropkin (4) have reported a relationship between convection coefficient h and extrapolated superheat-layer thickness δ . In Figure (15) all the experimental data from the present work have been plotted in a similar manner. Marcus and Dropkin

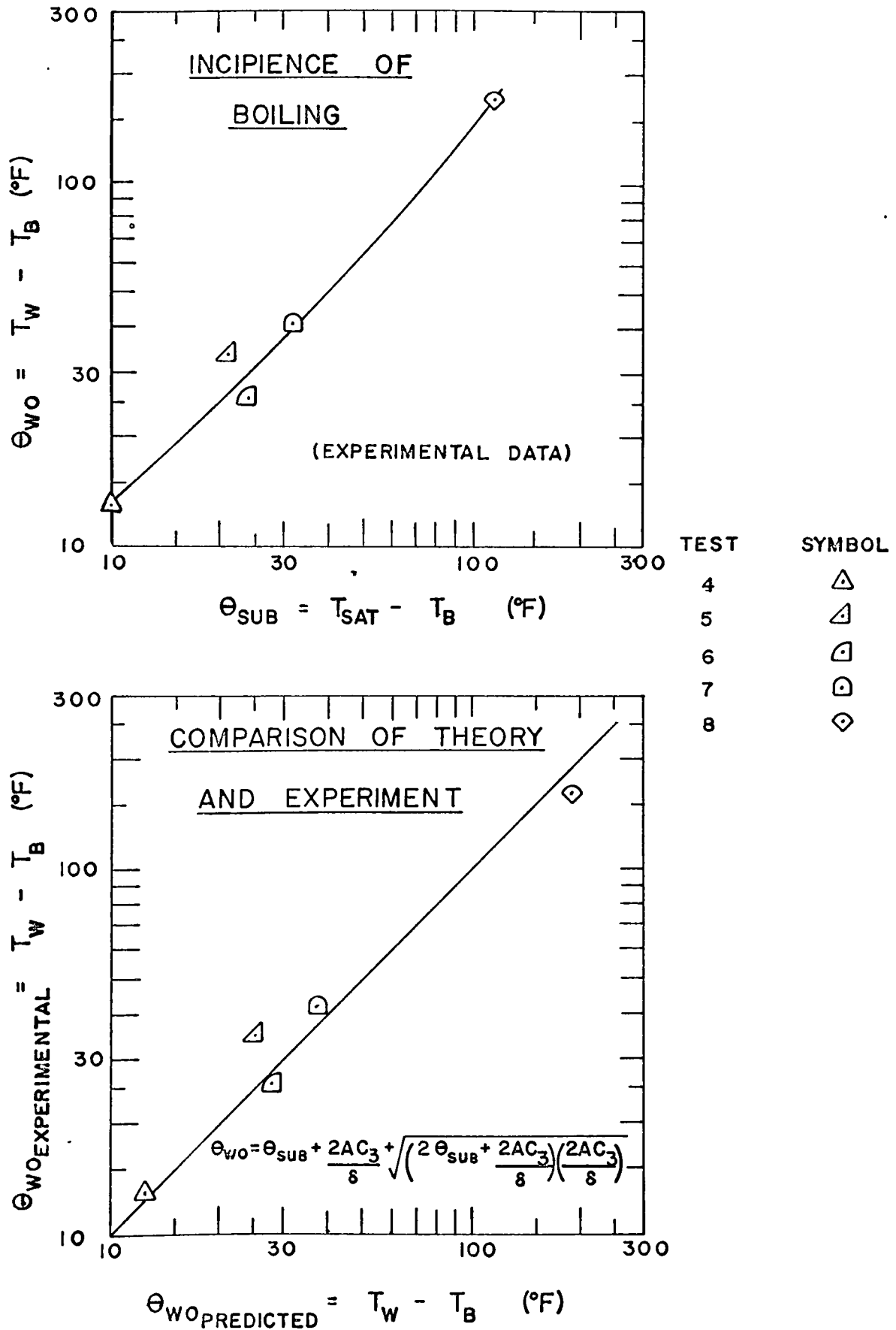


Figure 14 Incipience of Boiling Heat Transfer Data

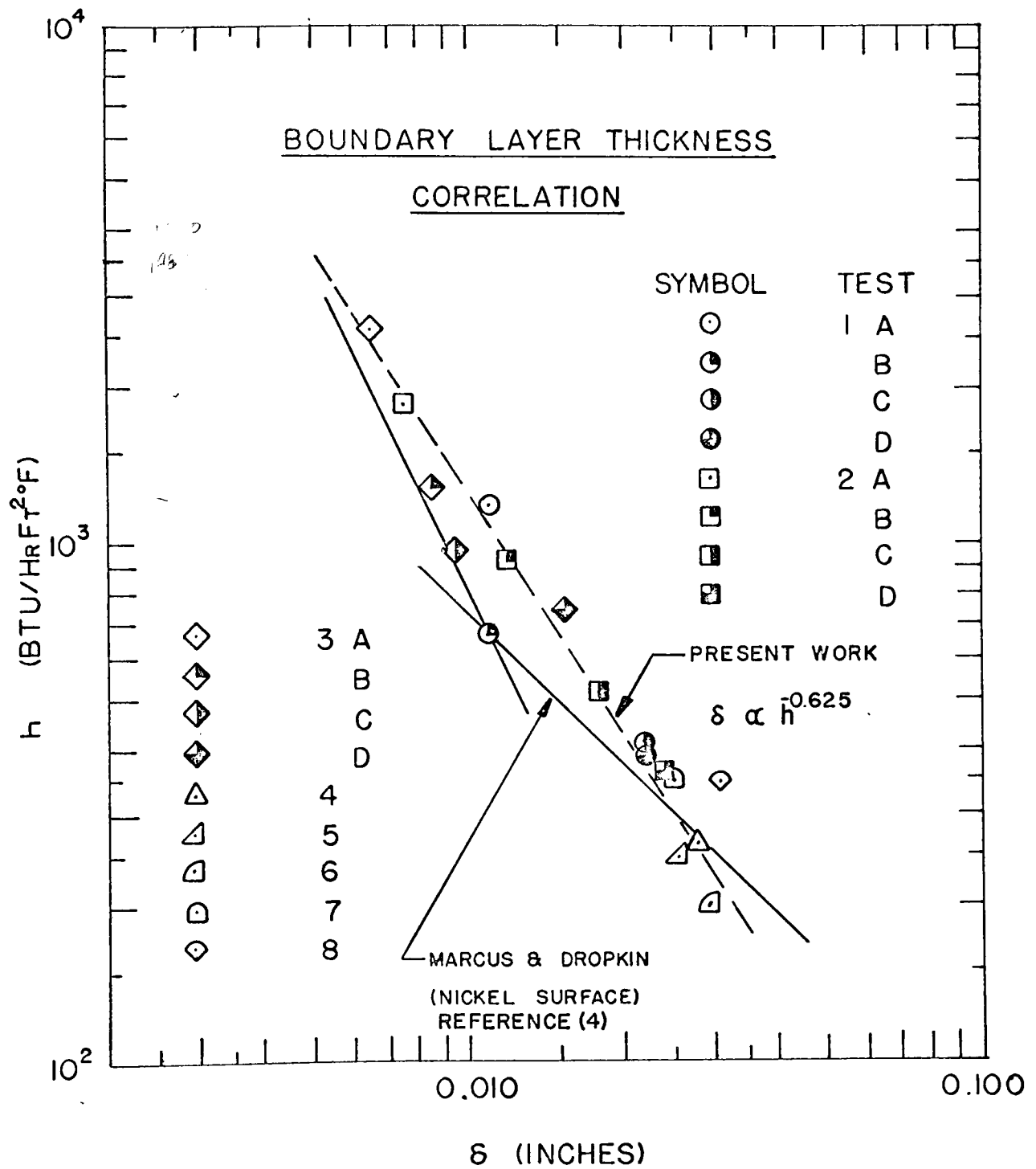


Figure 15 Boundary Layer Thickness Correlations

correlated data for saturated boiling into two regimes; $\delta \propto h^{-1}$ for the discrete bubble region where $h < 650$ BTU/HRFT² and $\delta \propto h^{-1/2}$ for the first transition region where $650 < h < 3000$ BTU/HRFT². The data from the present investigation has been correlated by a single relationship $\delta \propto h^{-0.625}$. It should be noted that while Marcus and Dropkin correlated data for saturated boiling only, the relationship $\delta \propto h^{-0.625}$ satisfactorily correlates data from both saturated and subcooled boiling. In general δ decreases with increasing h . Marcus and Dropkin note that in this sense the superheated boundary layer can be thought of as a "resistance barrier" to heat transfer between the heating surface and the bulk liquid, a thinner "barrier" corresponding to a higher heat transfer coefficient.

Chang (13) has proposed an equivalent conduction analogy for natural convection and nucleate boiling from a heated horizontal plate facing upward. In essence, Chang replaced the thermal conductivity K by an effective thermal conductivity K_{eff} in the Fourier conduction equation. That is

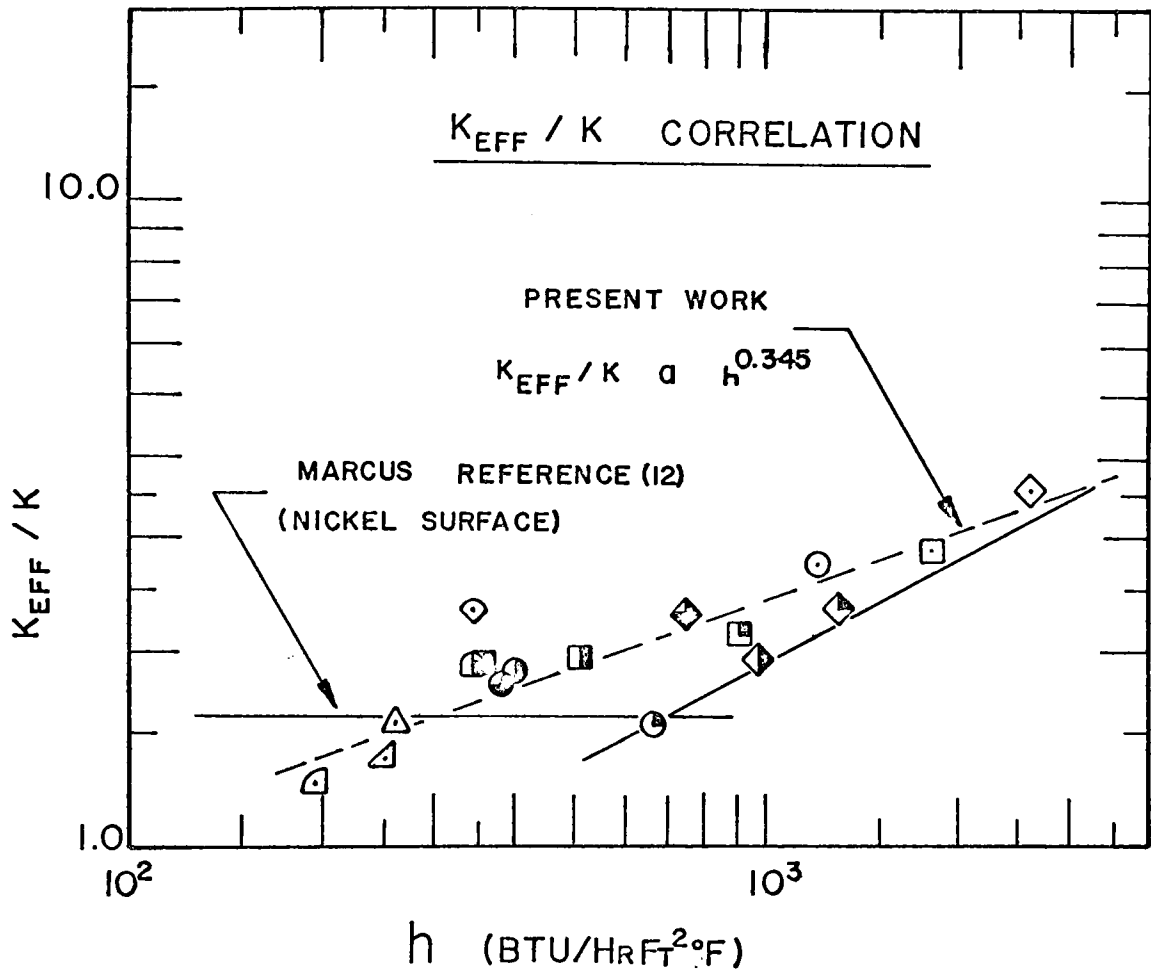
$$Q/A = - K_{eff} \left. \frac{dT}{dz} \right|_{z=0} \quad (10)$$

The temperature gradient in the water near the surface is taken as $\left. \frac{dT}{dz} \right|_{z=0}$. In view of the definition of

the extrapolated superheat-layer thickness, the temperature gradient in the liquid near the surface can be replaced by θ_w/δ both of which have been experimentally determined. Figure (16) shows the present work superimposed on the work of Marcus (12). Of significance is the fact that in all tests, K_{eff}/K is greater than unity. From this fact, it is apparent that the turbulence and mixing in the bulk liquid caused by natural convection and bubble motion increases the effective thermal conductivity and hence increases the heat transfer from the boiling surface to the bulk liquid. As in the correlation of δ versus h , all the data (saturated and subcooled boiling) can be correlated by a single relationship of the form $K_{eff}/K \propto h^{0.345}$.

When comparing the data of Marcus (12) and Marcus and Dropkin (4) to the present work, it is important to note in the first case water was boiled on a nickel surface while a copper surface was used in the latter case.

The fact that one correlation seems to draw all the data together for the two analyses mentioned, irrespective of the level of heat flux or subcooling, would indicate that the mechanism of heat transfer with a subcooled bulk liquid is similar to that of low heat



SYMBOL	TEST	SYMBOL	TEST
○	1 A	◇	3 A
⊙	B	◊	B
⊖	C	◈	C
⊗	D	◉	D
□	2 A	△	4
◻	B	▴	5
◼	C	◡	6
◽	D	◢	7
		◣	8

Figure 16 K_{eff}/K Correlation

flux saturated boiling. Visual observations of boiling in these two conditions would lend support to this hypothesis. It was noticed that in both cases the bubbles departing from the boiling surface were small in size and strong convection currents were evident.

After all the tests were completed the R.M.S. roughness of the surface was measured as approximately 20 to 25 micro inches. Noting that the initial surface roughness was approximately 5 micro inches, it is apparent that the boiling action changed the surface condition in some way.

This study presents a comprehensive set of measurements showing the effect of heat flux and subcooling on temperature profiles taken in the thermal boundary layer for water boiling on a copper surface. In addition, tests were performed to acquire data at the incipience of boiling. To the author's knowledge, many of the measurements taken have not been previously reported in the literature.

The results of the present study indicate that increasing heat flux and decreasing the level of subcooling have the effect of decreasing the thermal boundary layer thickness. Hsu's mathematical model for nucleation was tested using the incipient boiling condition at five levels of subcooling. Although not conclusive, the tests lend support to this model.

10.

NOMENCLATURE

<u>ARABIC SYMBOLS</u>	<u>DESCRIPTION</u>	<u>UNITS</u>
A	Area	FT ²
A	In Equation (4) and (5), a parameter representing $2\sigma T_{\text{sat}}/h_{\text{fg}}\rho_v$	FT°R
C ₁	Constant; 2	-
C ₃	Constant; 1.6	-
C _d	Drag coefficient	-
C _p	Specific heat	BTU/lbm
D	Diameter	FT
d	Deflection	in.
F	Force	lbf
g _o	Gravitational constant	lbmft/lbfsec ²
h _{fg}	Latent heat of vapourization	BTU/lbm
h	Heat transfer coefficient	BTU/HRFT ² °F
j	Parameter representing $(hP/KA)^{1/2}$	- 1/FT
K	Thermal conductivity	BTU/HRFT°F
L	Length, thickness	FT
m	Mass	lbm
m	In Equation (A-2) parameter representing $(2h_c/Kt)^{1/2}$	1/FT

N	Turns differential lead screw shaft	-
P	Pressure	lbf/in ²
ΔP	Pressure difference	lbf/in ²
Q	Rate of heat transfer	BTU/HR
r_c	Cavity radius	in.
$r_{1,2}$	Inner, outer radius	in.
R	Result	-
T	Temperature	°F
t	Thickness, equation (A-2)	in.
t	Time, equation (D-2)	sec.
v	Specific volume	FT ³ /lbm
V	Velocity	FT/sec
V_n	n'th variable	-
W_n	Uncertainty in n'th variable	-
W_R	Uncertainty in result	-
X	Length of span	in.
Z	Distance from probe thermocouple to boiling surface	in.
Z_o	Distance between tip of positioning needle and probe thermocouple	in.

Greek Symbols

δ	Limiting thermal layer thickness Han and Griffith, Reference (11)	in.
η_f	Fin effectiveness	
θ_{sub}	Subcooling ($T_{sat} - T_b$)	$^{\circ}F$
θ_w	Superheat ($T_w - T_{sat}$)	$^{\circ}F$
θ_{wo}	Incipient superheat ($T_{wo} - T_{sat}$)	$^{\circ}F$
ϵ	Limiting thermal layer thickness Yamagata, Reference (10)	in.
ρ	Density	lbm/FT ³
σ	Surface tension	lbf/FT

Subscripts

A	Ambient
b	Bulk
C	Convection
D	Drag
E_{ff}	Effective
f	Final
H	Heater
i	Initial, inner
junc	Junction
l	liquid
o	outer

s	Surface
sup	Superheated
sub	Subcooled
sat	Saturation
T	Tension
v	Vapour
w	Wall
w ₀	Wall, incipience of boiling

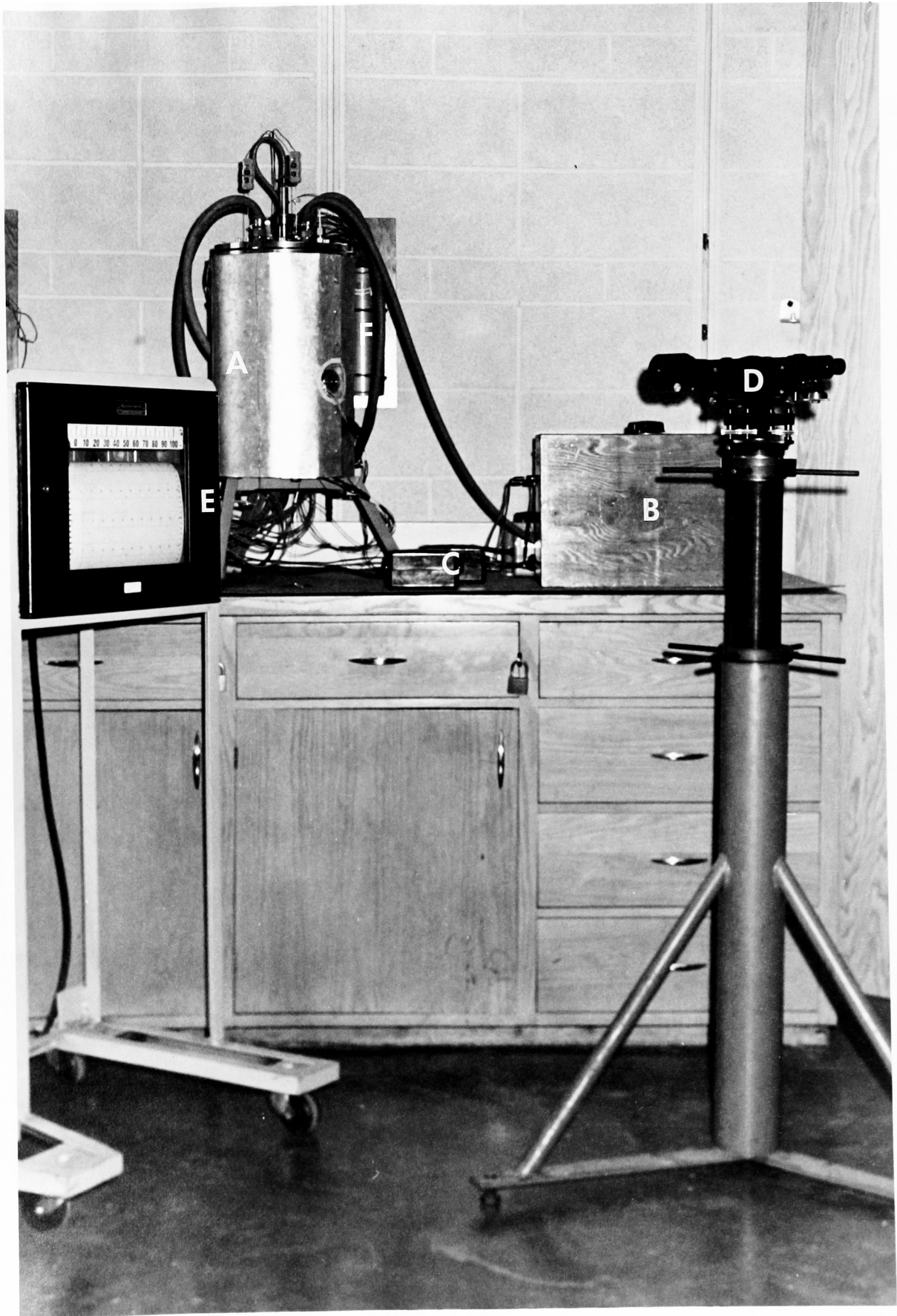


Figure 17 Test Facility

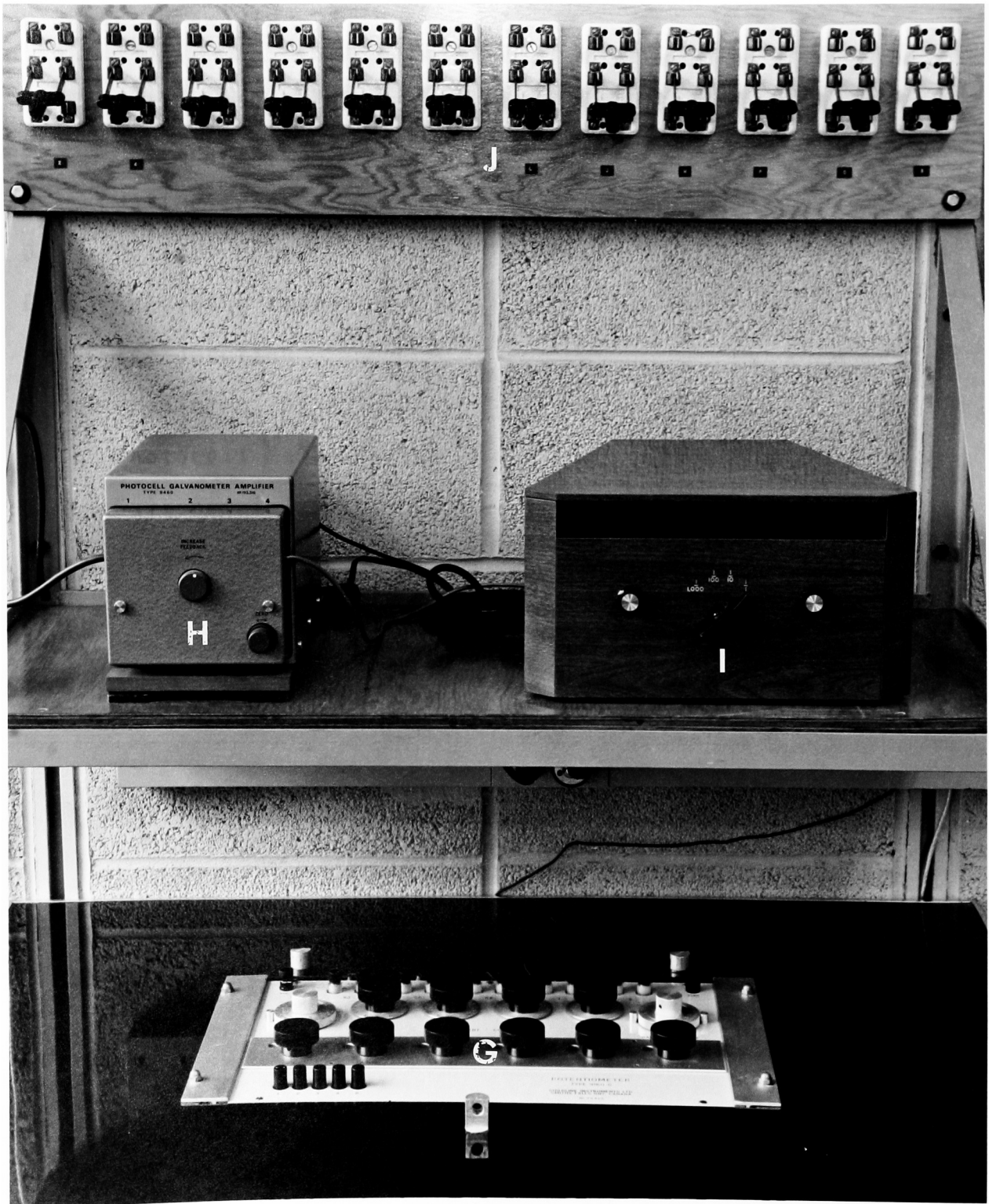


Figure 18 Precision Potentiometer and Related Instruments

FIGURES 17 AND 18

- A Boiler Assembly
- B Autotransformer
- C Wattmeters
- D Optical Level
- E Recording Potentiometer
- F Ice Junction
- G Precision Potentiometer
- H Photocell Galvanometer Amplifier
- I Galvanometer
- J Thermocouple Switchboard

1. Jakob, M., Heat Transfer, John Wiley & Sons, 1949.
2. Griffith, P., and Wallis, J., "The Role of Surface Conditions in Nucleate Boiling", C.E.P. Symposium Series, Number 30, Vol. 56, 1960.
3. Hsu, Y.Y., "On the Size Range of Active Nucleation Cavities on a Heating Surface", Transactions A.S.M.E. Journal of Heat Transfer, Series C, Vol. 84, 1962.
4. Marcus, B.D., and Dropkin, D., "Measured Temperature Profiles Within the Superheated Boundary Layer Above a Horizontal Surface in Saturated Nucleate Pool Boiling of Water", Transactions of the A.S.M.E. Journal of Heat Transfer, Series C, Volume 87, No. 3, 1965.
5. Lippert, T.E., and Dougall, R.S., "A Study of the Temperature Profiles Measured in the Thermal Sublayer of Water, Freon 113 and Methyl Alcohol During Pool Boiling", Transactions of the A.S.M.E. Journal of Heat Transfer, Series C, Vol. 90, 1968.
6. Bobst, R.W., and Colver, C.P., "Temperature Profiles up to Burnout Adjacent to a Horizontal Heating Surface in Nucleate Pool Boiling Water", C.E.P. Symposium Series, Volume 64, No. 82, 1968.
7. Judd, R.L., "Influence of Acceleration on Subcooled Nucleate Boiling", Ph.D. Thesis, The University of

Michigan, Ann Arbour, Michigan, 1968.

8. Gilb, G.H., Marcus, B.D., and Dropkin, D., "On the Manufacture of Fine Wire Thermocouple Probes", Review of Scientific Instruments, Volume 35, No.1, 1964.
9. Gaertner, R.F., "Photographic Study of Nucleate Pool Boiling on a Horizontal Surface", Transactions of the A.S.M.E. Journal of Heat Transfer, Series C, Volume 87, No.1, 1965.
10. Yamagata, K., Hirono, R., Nishikawa, K., and Matsuoka, H., "Nucleate Boiling of Water on the Horizontal Heating Surface", Mem. Faculty of Engineering Kyushu, 15, No.1, 1955.
11. Han, C.Y., and Griffith, P., "The Mechanism of Heat Transfer in Nucleate Pool Boiling", International Journal of Heat and Mass Transfer, Vol. 8, 1965.
12. Marcus, B.D., "Experiments on the Mechanism of Saturated Nucleate Pool Boiling Heat Transfer", Ph.D. Thesis, Cornell University, Ithaca, N.Y., June, 1963.
13. Chang, Y.P., "A Theoretical Analysis of Heat Transfer in Natural Convection and in Boiling", Transactions A.S.M.E., 79, 1957.
14. Schinck, H., Heat Transfer Engineering, Prentice-Hall, Inc., 1959.

15. Kreith, F., Principles of Heat Transfer, International Textbook Company, 1965.

APPENDIX A
ESTIMATE OF HEAT LOSS

The usual manner for determining the heat flux from a boiling surface in an apparatus such as that used in the present work is to measure the axial temperature distribution in the copper block near the surface and to use the Fourier conduction equation in conjunction with the axial temperature gradient to calculate Q/A assuming one dimensional conduction along the axis. Only after several boiling tests had been made with the apparatus was it discovered that the copper heating block had a thermal conductivity considerably less than that of pure copper, apparently as a result of being cast from a commercial grade copper ingot. As a consequence, an accurate value for the thermal conductivity of the heating block material was not known and the Fourier conduction equation could not be used to evaluate the heat flux.* As an alternative method for determining the heat flux, a heat balance was performed on the heater block in a manner described in detail below.

* Using the values of heat flux calculated from heat loss considerations, the thermal conductivity of the heater block material was calculated to be approximately 145 BTU/HRFT°F.

A series of tests in which water was boiled at saturated conditions through a range of input power settings (100 watts to 1200 watts) was performed to determine the temperature distribution in the copper block and surrounding insulation. With this information an initial estimate of heat loss from the heater assembly was made using the equations developed later in this section. A plot of the axial temperature gradient versus the initial heat flux estimate is seen to yield the "initial correction curve" in Figure (19). It is important to notice that the points fall essentially in a straight line which fails to pass through the origin by an offset of approximately $3^{\circ}\text{F}/\text{inch}$. The small offset suggests that although the assumption of one dimensional heat conduction is correct, the evaluation of the heat flux at the lower heat values is in error since the presence of an axial temperature gradient in the heater with no heat transfer is an impossibility. By a study of the temperature distribution in the vermiculite it was decided that the mathematical model used in calculating heat loss, which assumed radial heat loss to be predominant, was most nearly correct at a heat flux of approximately $100,000 \text{ BTU}/\text{HRFT}^2$. It was noticed that at low heat fluxes

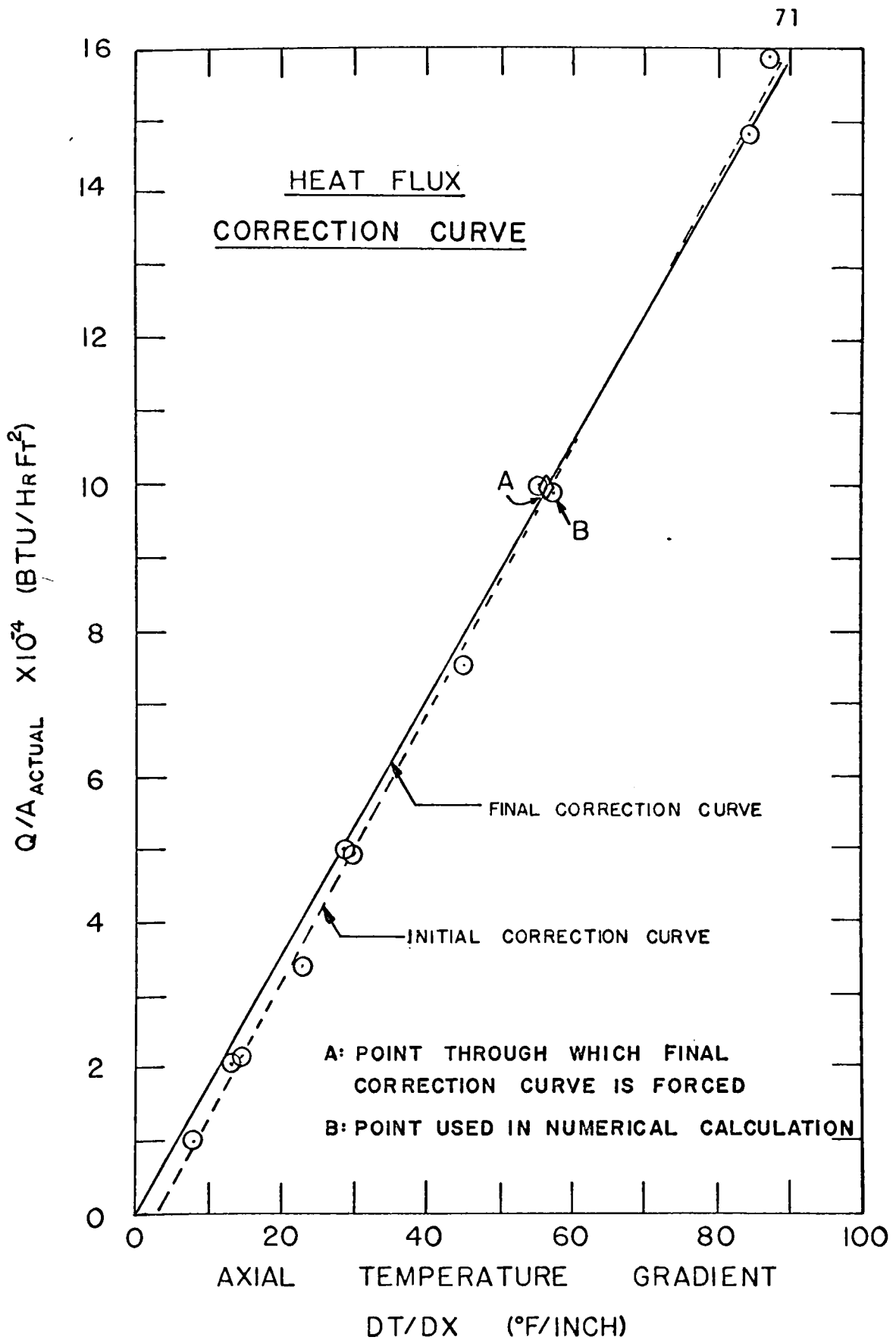


Figure 19 Heat Flux Correction Curve

the radial temperature gradient in the vermiculite was low in relation to the axial gradient in the vermiculite and hence the values of heat loss calculated at this condition were susceptible to large error. On this basis, the "final correction curve" was obtained by rotating the "initial correction curve" about point A as seen in Figure (19) until it passed through the origin. The final and initial correction curves are seen to be very close. Using the final correction curve the actual heat flux from the boiling surface can be determined from a measurement of the axial temperature gradient in the neck of the heating block. A sample of the heat loss calculations is presented below.

SAMPLE HEAT LOSS CALCULATIONS

SKIRT HEAT LOSS: -

The following assumptions were made in evaluating heat loss from the skirt:

1. The skirt acted as a circumferential fin.
2. The bottom face is considered to be an adiabatic plane.
3. Heat loss from the edge of the skirt at the flange is neglected.

The heat loss contribution of the skirt was calculated

by the relationship

$$Q_{fin} = \eta_f \bar{h}_c A (T_{Fin\ Base} - T_b) \quad (A-1)$$

in which the fin effectiveness η_f is given by

$$\eta_f = f(m, L) = f\left(\sqrt{\frac{2h_c}{Kt}}, L\right) \quad (A-2)$$

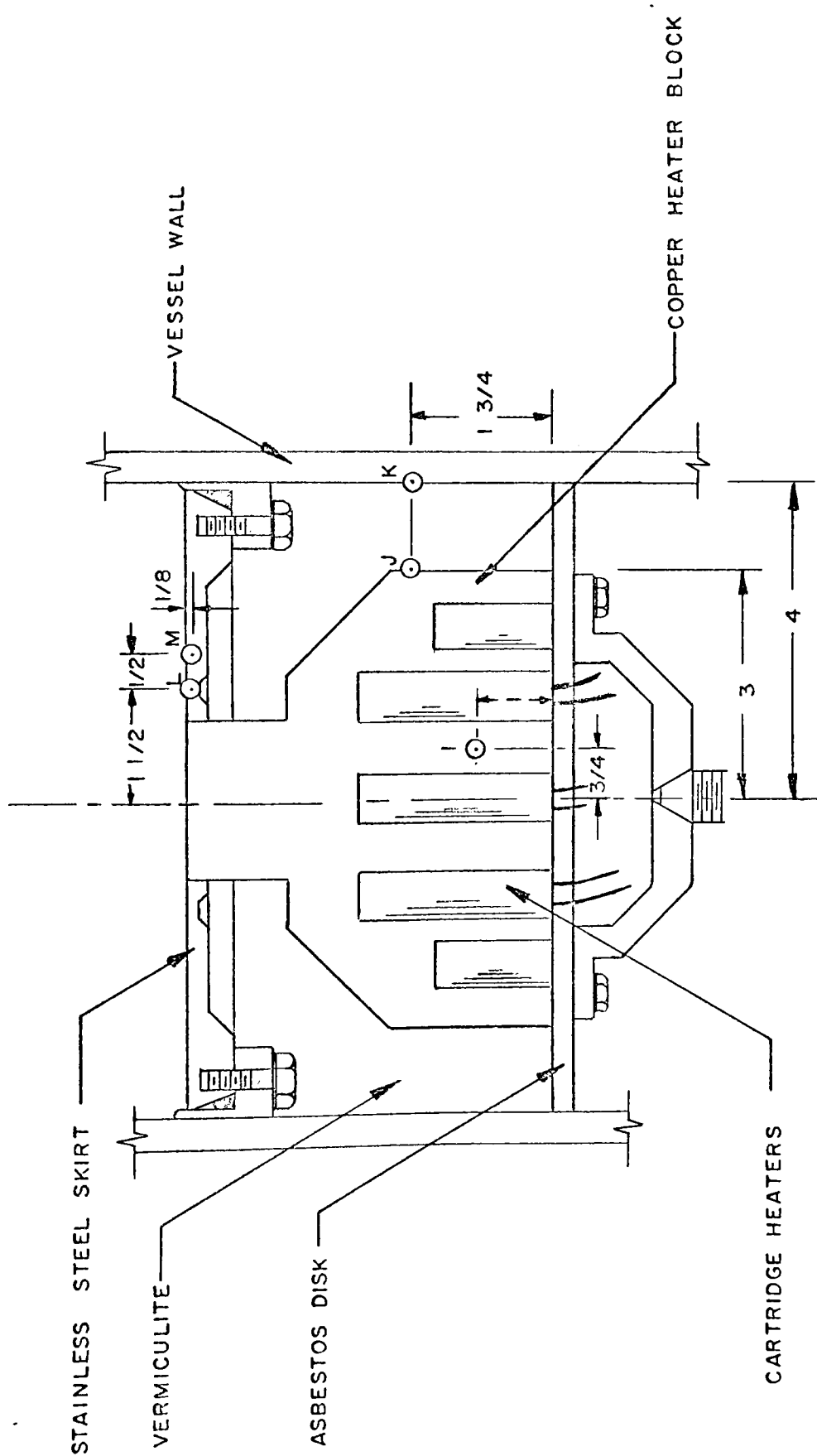
The functional relationship between η_f and mL is given in Schenck(14).

Upon substitution of $\bar{h}_c = 130 \text{ BTU/HRFT}^2\text{°F}$, $K = 9.2 \text{ BTU/HRFT}^2\text{°F}$, $t = 0.5 \text{ inch}$, $D_o = 7.75 \text{ inch}$, $D_i = 2 \text{ inch}$ and $L = 2.88 \text{ inch}$, $mL = 6.25$ is obtained. Then $\eta_f \approx 0.085$ and by definition

$$Q_{fin} = 3.36 (T_{Fin\ Base} - T_b) \text{ BTU/HR} \quad (A-3)$$

RADIAL HEAT LOSS THROUGH VERMICULITE:

In calculating the heat lost from the heater block through the vermiculite, it was assumed that the temperature distributions in the vermiculite were essentially radial in nature. Figure (20) shows that the volume occupied by the vermiculite can be considered to be two cylinders for the purpose of analysis; one around the neck of the heater block, the other around the base of the heater block. In both cases, the well known equations for radial heat transfer through a hollow cylinder apply.



(ALL DIMENSIONS NOMINAL) (●) THERMOCOUPLE

Figure 20 Location of Thermocouples used in Determining Heat Loss

$$Q = \frac{2\pi K_v L}{\ln\left(\frac{r_2}{r_1}\right)} (T_1 - T_2) \quad (\text{A-4})$$

Upon substituting values of $K_v = 0.48$ BTU/HRFT $^\circ$ F, $L = 1$ inch, $r_2 = 4$ inch and $r_1 = 1$ inch in Equation (A-4) an expression for the radial heat loss from the neck of the heater block Q_{v1} is obtained.

$$Q_{v1} = 0.18 (T_1' - T_2) \text{ BTU/HR} \quad (\text{A-5})$$

T_1' is estimated from thermocouple F and T_2 is measured by thermocouple K. Using values of $K_v = 0.48$ BTU/HRFT $^\circ$ F, $L = 4$ inch, $r_2 = 4$ inch and $r_1 = 3$ inch in Equation (A-4) results in an expression for radial heat loss from the base of the heater block, Q_{v2} .

$$Q_{v2} = 2.62 (T_1 - T_2) \text{ BTU/HR} \quad (\text{A-6})$$

T_1 and T_2 are measured by thermocouples J and K, respectively.

HEAT LOSS FROM THE BOTTOM FACE OF HEATER BLOCK:

An asbestos disk 1/4 inch thick was fixed to the bottom of the heater block to reduce heat transfer in that direction as well as hold the vermiculite in place. The heat loss Q_b becomes:

$$Q_b = \frac{T_h - T_a}{\frac{L}{KA} + \frac{1}{R_c A}} \quad (\text{A-7})$$

Substituting values of $L = 0.25$ inch, $A = 0.34$ FT²,
 $K = 0.09$ BTH/HRFT°F, using $\bar{h}_c = 0.12 \left(\frac{T_s - T_a}{D} \right)^{1/4}$
 (Schenck (14)) and $D = 0.66$ FT. Equation (A-7)
 becomes

$$Q_b = \frac{(T_h - T_a)}{0.6 + \frac{22}{(T_s - T_a)^{1/4}}} \text{ BTU/HR} \quad (\text{A-8})$$

T_h and T_s are estimated from thermocouple I.

NUMERICAL CALCULATION

The following is a heat loss calculation to illustrate the use of the equations developed above. The data given below corresponds to point B in Figure (19).

$$Q_{\text{input}} = 716 \text{ watts} = 2440 \text{ BTU/HR}$$

THERMOCOUPLE	TEMPERATURE (°F)
A	260.4
B	282.7
C	303.8
D	283.5
E	283.8
F	284.0
G	211.7
H	211.7
I	358.0
J	336.5
K	209.8
L	214.9
M	214.6

$$Q_{fin} = 3.36 (T_{fb} - T_b) \text{ BTU/HR} \quad (\text{A-3})$$

$T_{fb} = 253.0^\circ\text{F}$ - extrapolation of axial temperature gradient to the elevation of the skirt centerline.

$T_b = 211.7^\circ\text{F}$ - thermocouples G and H

$$Q_{fin} = 3.36 (253.0 - 211.7) = \underline{139} \text{ BTU/HR}$$

$$Q_{v1} = 0.18 (T_1' - T_2) \text{ BTU/HR} \quad (\text{A-5})$$

$T_1' = 284.0^\circ\text{F}$ - thermocouple F

$T_2 = 209.8^\circ\text{F}$ - thermocouple K

$$Q_{v1} = 0.18 (284.0 - 209.8) = \underline{14} \text{ BTU/HR}$$

$$Q_{v2} = 2.62 (T_1 - T_2) \text{ BTU/HR} \quad (\text{A-6})$$

$T_1 = 336.5^\circ\text{F}$ - thermocouple J

$T_2 = 209.8^\circ\text{F}$ - thermocouple K

$$Q_{v2} = 2.62 (336.5 - 209.8) = \underline{332} \text{ BTU/HR}$$

$$Q_b = \frac{(T_h - T_a)}{0.6 + \frac{22}{(T_s - T_a)^{1/4}}} \text{ BTU/HR} \quad (\text{A-8})$$

$T_h = 358.0^\circ\text{F}$ - thermocouple I

$T_a = 75^\circ\text{F}$ - ambient temperature

$T_s = 330.0^\circ\text{F}$ - trial and error estimate

$$Q_b = \frac{(358.0 - 75.0)}{0.6 + \frac{22}{(330.0 - 75.0)^{1/4}}} = \underline{46} \text{ BTU/HR}$$

$$Q_{\text{LOSS}} = Q_{\text{fin}} + Q_{\text{v1}} + Q_{\text{v2}} + Q_{\text{b}}$$

$$Q_{\text{LOSS}} = \underline{531} \text{ BTU/HR}$$

For heat flux

$$\left(\frac{Q}{A}\right)_{\text{ACTUAL}} = \left(\frac{Q}{A}\right)_{\text{INPUT}} - \left(\frac{Q}{A}\right)_{\text{LOSS}} \quad (6)$$

where $A = 0.0195 \text{ FT}^2$, area of boiling surface

$$\left(\frac{Q}{A}\right)_{\text{ACTUAL}} = \frac{2440}{0.0195} - \frac{531}{0.0195}$$

$$\left(\frac{Q}{A}\right)_{\text{ACTUAL}} = \underline{98,000} \text{ BTU/HRFT}^2$$

APPENDIX B

EXTRAPOLATION OF THE AXIAL TEMPERATURE GRADIENT IN THE HEATER BLOCK

An important parameter in the study is the temperature of the boiling surface, T_w . As stated previously, this temperature was derived by extrapolating the temperature gradient measured by thermocouples A, B and C to the surface. It was felt that in order to provide some check on the locations of the thermocouples which has importance in the evaluation of surface temperature and heat flux, the surface temperature should be measured independently and compared to the extrapolated value. Adding to the importance of the test was the fact that the thermal conductivity of the heater block material was not known with any accuracy so that it was not known whether the extrapolation was reasonable or not.

A chromel-constantan thermocouple of 0.001 inch diameter wire was located on the surface to measure T_w . To induce a gradient in the heater block of sufficient magnitude for precise measurement, a jet of air was blown normal to the boiling surface. With an input

of 100 watts to the electrical heaters, a gradient of 5.1 °F/inch was established in the neck of the heater block. For this condition, the 0.001 inch thermocouple measured T_w as 223.5°F which compared favourably with the extrapolated value of 224.2°F. This close agreement gave confidence to the extrapolation procedure determining T_w .

APPENDIX C

BULK LIQUID TEMPERATURE

Early in the investigation it was realized that while the temperature in the bulk liquid was essentially constant for saturated boiling, a significant variation was present in a subcooled boiling condition. The temperature taken as being characteristic of the bulk liquid is important in that it describes the level of subcooling and hence has a direct bearing on calculated values of h , K_{eff}/K , θ_{w0} and the measurement of δ . Figure (21) shows three temperature profiles taken in a highly subcooled boiling liquid. As seen in the figure, the temperature of the liquid in the immediate vicinity of the surface is suppressed with respect to the bulk temperature while the temperature on the centerline above the boiling surface is high relative to the bulk temperature. At a displacement from the surface of approximately 2 inches, all three temperature profiles approach a common value of 118°F. On this basis, it was felt that the bulk temperature measured at a displacement of 2 inches sufficiently characterized the overall bulk temperature to warrant its use as a measure of the level of subcooling.

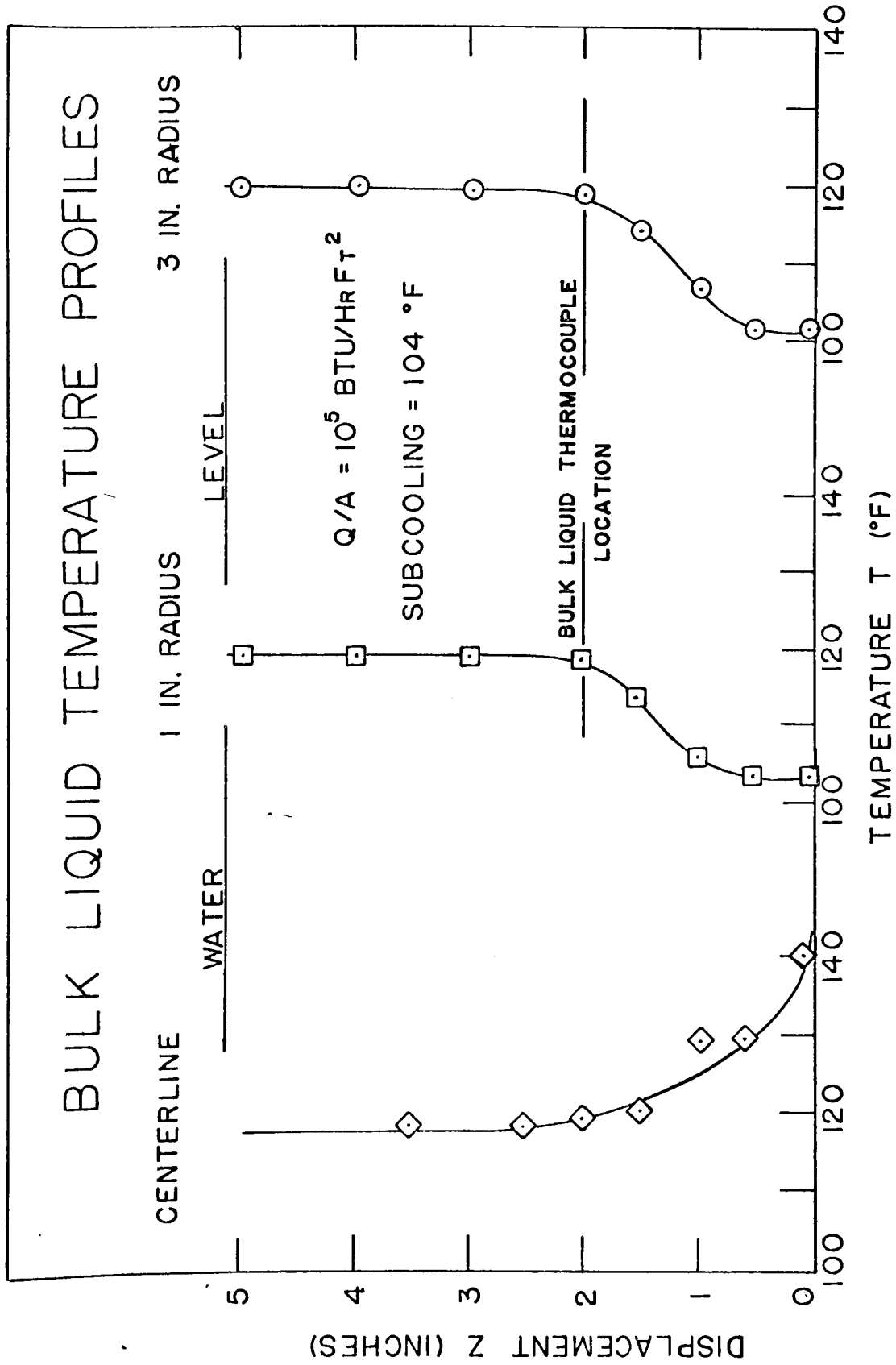


Figure 21 Bulk Liquid Temperature Profiles.

APPENDIX D

DESIGN OF THE THERMOCOUPLE PROBE

The problem of measuring a temperature profile within a thin superheated boundary layer above a boiling surface required a very careful design of the micro-thermocouple probe. In particular, the probe had to be small enough to provide adequate resolution of the temperature distribution; it had to have a response time small enough so that it could follow the temperature fluctuations; and it had to be designed so that it introduced minimum thermocouple error. The final design included these considerations.

I RESPONSE TIME OF THE THERMOCOUPLE PROBE TO A STEP CHANGE IN THE ENVIRONMENTAL TEMPERATURE.

To estimate the response time of the probe, the thermocouple bead can be treated as an isothermal sphere of 0.0025 inch diameter. A heat balance on the sphere yields:

$$Q = hA (T_f - T) = m C_p \frac{dT}{dt} \quad (D-1)$$

The solution of Equation (D-1) after substituting initial conditions is

$$\frac{T - T_f}{T_i - T_f} = \exp \left(\frac{-6ht}{\rho DC_p} \right) \quad (D-2)$$

A conservative estimate of h can be obtained by considering the junction bead heated (or cooled) by natural convection. Such an assumption yields:

$$h \approx 550 \text{ BTU/HRFT}^2\text{ }^\circ\text{F} \quad (\text{D-3})$$

If the response time is considered to be the time required for the bead to attain 95% of the step change in the environmental temperature, Equation (D-2) yields:

$$t_{95\%} = 0.030 \text{ sec.}$$

Thus, the probe could follow temperature fluctuations in the order of 35 cps before the error became appreciable. As the maximum fluctuation frequency encountered was in the order of 10 cps, the temperature response of the probe was more than adequate.

2 RESOLUTION OF THE THERMOCOUPLE PROBE

It is necessary to estimate the accuracy with which the probe and traversing mechanism measured the displacement z from the surface.

The traversing mechanism described in section 3.4 was found to reproduce settings within 0.0003 inch and thus provided very little error. Of greater importance is an estimate of the static deflection of the suspended thermocouple junction.

The deflection was considered to be caused by

the drag force of water flowing over the wire. The drag force is given by

$$F_d = \frac{C_d \rho V^2 A}{2g_o} \quad (D-4)$$

Upon substituting in values of $C_d = 1.6$ (reference (15)), $V = 5$ FT/SEC (reference (12)), $\rho = 60.1$ lbm/FT³ and $A = 0.0005$ in², Equation (D-4) yields

$$F_d = 0.26 \times 10^{-3} \text{ lb/inch of wire} \quad (D-5)$$

Considering the suspended wire as a cable in tension between two rigid supports acted upon by a uniformly distributed load according to Equation (D-5) yields Equation (D-6) for the maximum deflection

$$d_{\max} = \frac{F_d X^2}{8 F_T} \quad (D-6)$$

For the probe of $X = 1/2$ inch it was desired to limit the junction deflection to approximately 0.0003 inch. Upon substituting these values into Equation (D-6)

$$F_T = 0.027 \text{ lbf} \quad (D-7)$$

A tension of approximately 0.027 lbf was introduced in the wire by hanging sufficient weight on the wire and "springing" the glass capillary tubes before cementing the wire in place with epoxy.

3 THERMOCOUPLE ERROR

An estimate of the effect of conduction along

the thermocouple leads on the junction temperature (T_{junc}) is made in this section. A conservative estimate for the thermocouple error is obtained if the probe wire is treated as a rod in a uniform temperature field (T_{sup}) with heat sinks at each end which are at the bulk temperature (T_b).

The solution of this problem is given by Jakob (1) as

$$T_{\text{sup}} - T_{\text{junc}} = \frac{(T_{\text{sup}} - T_b)}{\cosh\left(\frac{jx}{2}\right)} \quad (\text{D-8})$$

$$\text{where } j = \left(\frac{hP}{KA}\right)^{1/2} \quad (\text{D-9})$$

As shown in the estimate of thermocouple response time, the coefficient of heat transfer is in the order of 550 BTU/HRFT²°F. By using the conductivity of Constantan ($K = 12$ BTU/HRFT°F) (which is higher than that for Chromel) in calculating j

$$j = 1480 \text{ 1/FT and}$$

$$T_{\text{sup}} - T_{\text{junc}} = \frac{(T_{\text{sup}} - T_b)}{1.3 \times 10^{13}} \quad (\text{D-10})$$

Thus, the thermocouple error may be concluded to be negligible.

APPENDIX E

TABULATION OF DATA

TABLE II
SATURATED AND SUBCOOLED BOILING

Test	(Q/A) ACTUAL BTU/HRFT ²	T _{sat} °F	θ _w °F	θ _{sub} °F	δ inch	h BTU/HRFT ² °F	K _{eff} /K
1A	23,000	212.4	19.3	0.7	0.011	1190	2.76
B	23,000	212.3	34.9	15.7	0.011	660	1.53
C	23,000	212.3	57.2	41.5	0.022	400	1.87
D	21,500	212.5	56.9	52.9	0.022	380	1.78
2A	48,500	212.3	26.8	0.6	0.008	1810	2.88
B	53,500	212.3	59.0	33.2	0.012	910	2.31
C	46,500	212.2	91.5	67.3	0.018	510	1.95
D	44,500	212.3	124.0	105.3	0.024	360	1.84
3A	94,500	212.7	36.5	0.6	0.007	2590	3.55
B	94,500	212.5	73.0	32.7	0.009	1290	2.34
C	94,000	212.5	98.0	57.6	0.010	960	1.94
D	91,500	212.6	128.0	89.6	0.016	720	2.36
4	3,400	212.4	13.0	10.9	0.028	260	1.55
5	8,400	212.1	34.1	21.6	0.026	250	1.36
6	5,000	212.2	25.5	24.0	0.029	196	1.21
7	14,400	212.6	41.0	31.1	0.025	352	1.88
8	40,000	212.4	116.1	112.0	0.031	345	2.30

TABLE III

INCIPIENCE OF BOILING

Test	θ_{sat} (°F) Experimental	δ (in.)	θ_{wo} (°F) Experimental	θ_{wo} (°F)
4	10.0	0.028	13.0	12.5
5	21.1	0.026	34.1	24.8
6	24.0	0.029	25.5	27.8
7	32.1	0.025	41.0	36.7
8	112.0	0.031	116.1	119.5

APPENDIX F

UNCERTAINTY ANALYSIS

The following relationship was used to determine the uncertainty for each result computed

$$\frac{W_R}{R} = \left[\left(\frac{\partial R}{\partial V_1} \frac{W_1}{R} \right)^2 + \left(\frac{\partial R}{\partial V_2} \frac{W_2}{R} \right)^2 + \dots + \left(\frac{\partial R}{\partial V_n} \frac{W_n}{R} \right)^2 \right]^{1/2} \quad (F-1)$$

where R is the result, W_R is the uncertainty in the result, V_n is the n^{th} variable and W_n is the uncertainty in the n^{th} variable.

The value of W_R/R given by Equation (F-1) represents the root mean square uncertainty in the computed result.

The uncertainty in the calculated value of $\left(\frac{Q}{A}\right)_{\text{ACTUAL}}$ was 9.5%, in θ_{w0} was 6.1% while that for δ was 5%.

TABLE IV

<u>Uncertainty Description</u>	<u>Uncertainty</u>
Heat Flux	
$(\frac{Q}{A})_{ACTUAL} = (\frac{Q}{A})_{INPUT} - (\frac{Q}{A})_{LOSS}$	
(a) <u>Heat Loss</u>	
$Q_{LOSS} = Q_{fin} + Q_{V1} + Q_{V2} + Q_B$	
Q_{fin} (139 BTU/HR)	8.5%
Q_{V1} (14 BTU/HR)	15.0%
Q_{V2} (332 BTU/HR)	9.9%
Q_B (46 BTU/HR)	10.1%
Q_{LOSS} (531 BTU/HR)	6.6%
(b) <u>Heat Input</u>	
$Q_{INPUT} = 3.414 \text{ W}$	
Q_{INPUT} (2440 BTU/HR)	1.5%
(c) <u>Actual Heat Flux</u>	
$(\frac{Q}{A})_{INPUT}$ (125,000 BTU/HRFT ²)	6.6%
$(\frac{Q}{A})_{LOSS}$ (27,000 BTU/HRFT ²)	8.3%
$(\frac{Q}{A})_{ACTUAL}$ (98,000 BTU/HRFT ²)	9.5%

Surface Superheat

$$\theta_w = T_w - T_{sat}$$

$$\theta_w (40.3^\circ\text{F}) \quad 1.7\%$$

Bulk Subcooling

$$\theta_{sub} = T_{sat} - T_b$$

$$\theta_{sub} (43.0^\circ\text{F}) \quad 1.7\%$$

Probe Displacement

$$z = z_o + N(0.00445)$$

$$z (0.025 \text{ in.}) \quad 4.1\%$$

Extrapolated Superheat-layer Thickness

$$\delta (0.025 \text{ in.}) \quad 5.0\%$$

Temperature From Micro Thermocouple

$$T (200.0^\circ\text{F}) \quad 5.0\%$$

Surface Superheat (Incipience Of Boiling)

$$\theta_{wo} = \theta_{sub} + \frac{2AC_3}{\delta} + \left[\left(2\theta_{sub} + \frac{2AC_3}{\delta} \right) \left(\frac{2AC_3}{\delta} \right) \right]^{1/2}$$

$$\theta_{wo} (38.1^\circ\text{F}) \quad 6.1\%$$

Heat Transfer Coefficient

$$h = \frac{(Q/A)_{actual}}{(T_w - T_b)}$$

$$h (352 \text{ BTU/HRFT}^2\text{ }^\circ\text{F}) \quad 11.6\%$$

K_{eff}/K Ratio

$$\frac{K_{eff}}{K} = \frac{(Q/A)_{actual} \delta}{K (T_w - T_b)}$$

$$\frac{K_{eff}}{K} \quad (1.88)$$

12.5%

